# Aerial Generalized Slung Load Transportation

Pedro O. Pereira and Dimos V. Dimarogonas

*Abstract*—This paper focuses on a pose tracking problem for a system composed of two connected rigid bodies, namely an aerial vehicle – with hovering capabilities, and a rod-like rigid body. The rod-like rigid body has an axis of axial symmetry, and the joint connecting the aerial vehicle and the rod lies somewhere along that axis. The aerial vehicle is meant to transport that object that can swing/slung with respect to the vehicle: we refer to *generalized* slung load transportation because the object being transported is a rod-like object, as opposed to *standard* slung load transportation where the object is a point mass with no moment of inertia. Given this system, we consider two tracking problems. Firstly, we assume that a torque input on the joint is available, and, for this scenario, we formulate a *semi*-pose tracking problem, requiring the rod object to track a desired pose trajectory, apart from rotations around its axis of axial symmetry (and thus the *semi* qualifier). Secondly, we assume that no such torque input is available, and, for this scenario, we formulate a position tracking problem, requiring a specific point along the axis of axial symmetry of the rod object to track a desired position trajectory. Our approach for solving both these problems lies in finding a state and an input transformations, such that the vector field in the new coordinates is of a known form for which controllers are found in the literature, and which we leverage in this paper. Simulations are presented to validate the proposed algorithms.

## I. INTRODUCTION

Unmanned aerial vehicles (UAVs) provide a platform for performing and testing a variety of tasks. Among other things, UAVs have been used to map large surface areas, surveil dangerous terrains, and inspect remote infrastructures [1]–[3]. More recently, UAVs with hovering capabilities have been successfully employed in transporting cargoes, which is of interest in dangerous and cluttered environments [4], [5].

Aerial transportation can be roughly categorized as slung-load/tethered-transportation [5]–[16] *vs* manipulator-endowed-transportation [3], [17]–[24]; and as single-UAV transportation *vs* (cooperative) multiple-UAV transportation. Slung-load/tethered transportation, when compared with transportation by manipulators, is mechanically simple, inexpensive, and it does not require any power supply; manipulator-endowed transportation, on the other hand, provides extra degrees of freedom which can be used to perform more complex tasks – such as picking up an object from inside a drawer [18]. In cluttered environments, transportation with a single UAV may be the only feasible option, while transportation with multiple UAVs is primarily necessary when the cargo exceeds the individual UAVs' payload capacity. In this paper, the system at study is composed of a single UAV connected to a rod-like object, and two different cases are considered: in the first case, we assume a torque input at the joint connecting the UAV

and the object is available, thus falling into the manipulator-endowed transportation – see Fig. 1a; in the second case, no such torque is made available, thus falling into the slung-load/tethered transportation – see Fig. 1b.

Different aspects of aerial transportation have been considered in the literature. In slung-load transportation, vision and force sensors has been used to estimate the swing angle of the load or to autonomously estimate the cargo's pose, and used in the feedback loop to avoid/dampen swing excitation [6]–[8], [25], [26]; in manipulator-endowed transportation, it has been used to correctly place end-effectors with respect to a visual target placed on the object to be transported [8], [26]–[28]. Differential flatness has been used for the purposes of control and motion planning [11], [21], [29]–[32], such as planning trajectories that minimize the loads' swing. Motion planning for collision avoidance between the cargo and the UAVs with obstacles in a cluttered environment has also been studied and validated [14], [19], [20], [33]. Adaptive and robust controllers have also been proposed, which estimate and compensate for the static and dynamic effects of the cargo on the UAV [5], [22]–[24].

In aerial tethered transportation, a cable establishes a physical connection between the UAV and the load, and, under tensile forces, it behaves like an un-actuated manipulator (i.e., like a rigid link). To be specific, under tensile forces, the cable imposes a holonomic restriction, namely that the distance between the UAV and the load is equal to the cable length; if that is not the case, no such restriction applies, and the UAV and the load can move independently. In the literature of tethered transportation, some works have focused on the hybrid modeling describing the dynamics when the cable is taut and when it is not, and hybrid controllers have also been proposed that deal with the hybrid dynamics [10], [11], [34]. In this paper, we model the rod-like object as a rigid three-dimensional pendulum that, rather than attached to a fixed pivot-point [35]–[37], is attached to a moving one, namely the UAV – see Fig. 1b. Because the rod is rigid, it can withstand compression forces, and the need for a hybrid model is unnecessary. Nonetheless, this paper's results apply for tethered transportation, provided that the cable remains under tensile forces.

### A. Paper's organization

In Section III, we briefly introduce some notions of rigid body kinematics and dynamics. In Section IV, we model our system composed of two rigid bodies, namely a UAV and a rod-like object. We consider two systems, one where there is a torque input at the joint connecting the rigid bodies – UAV-manipulator system (Fig. 1a); and one where there is not – UAV-slung-manipulator system (Fig. 1b). In Subsection IV-A, we formulate the problem statement for the UAV-manipulator system, and in Subsection IV-B, we formulate the

problem statement for the UAV-slung-manipulator system. In Section V, we explain the control strategy for both problems; and in Section VI, we implement that strategy for the UAV-manipulator system, while in Section VII we implement that same strategy for the UAV-slung-manipulator system. Finally, in Section VIII, we provide some illustrative simulations. In [49], one finds mathematica files that corroborate all the presented results.

### B. Contributions

Let us summarize some of this paper's contributions. First of all, we note that the considered system is not fully actuated, and thus inverse dynamics control – where a nonlinear control law linearizes and decouples the system [38] – cannot be implemented.

One of our contributions lies in analyzing two problems under a common framework: namely, we consider a UAV-manipulator system and a UAV-slung-manipulator system, which are the same system, with the exception that the UAV-slung-manipulator system is deprived of a torque input (and thus the *slung* in the naming).

Another main contribution, with respect to the UAV-manipulator system, lies in showing that it is equivalent to two decoupled subsystems: one concerning the position of the center-of-mass of the system, and another concerning the attitude of the manipulator. The first subsystem has the dynamics of a VTOL vehicle, and thus we are able to leverage controllers from the literature to control the position of the center-of-mass [39]–[42]. The second system has the dynamics of a second order system in the unit sphere, and thus we are able to leverage controllers from the literature to control the attitude of the manipulator [43]–[46].

Equivalently, another main contribution, this time with respect to the UAV-slung-manipulator system, lies in showing that it is equivalent to a VTOL vehicle cascaded after a second order system in the unit sphere. For this system, we are also able to leverage controllers for VTOL vehicles from the literature, which must be complemented with two backstepping steps (related to the second order system). We emphasize that this system is a generalization of the slung load system: indeed, rather than a point mass, the aerial vehicle carries a rigid body with some moment of inertia, with the slung load problem being recovered if that moment of inertia vanishes.

This work provides an extension of the results found in [47] and [48], the first related to manipulator-endowed transportation and the latter to slung transportation. This paper unifies those two problems, while generalizing them at the same time. To be specific, in [47] and [48], the load is taken to be a point-mass, whilst in this paper it is taken as a rod-like object with non-zero inertia. In order to analyze these two problems, and because the rod-like object has an axis of axial symmetry, we need to *ignore* the rotations of the rod object around that axis. This is done in a precise manner, by introducing an equivalence relation, and performing the analysis in the quotient space. This also constitutes anther contribution of this paper.
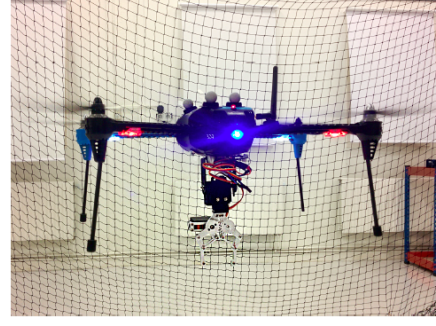


(a) Manipulator that can be modeled as a rod-like rigid body, and with a torque input available at the joint connecting the manipulator to the aerial vehicle.
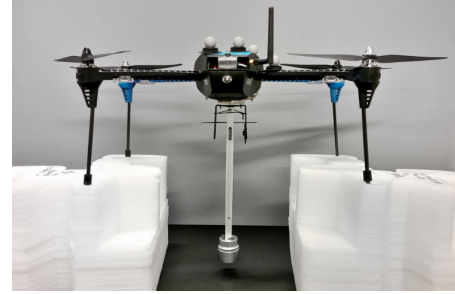


(b) A rod-like object connected to an aerial vehicle at a point along the axis of axial symmetry: the rod object may be interpreted as an un-actuated manipulator.

Fig. 1: Real system composed of an aerial vehicle (Iris+ from 3D Robotics) and a manipulator/rod-like-object.

## II. NOTATION

The map $\mathcal{S} : \mathbb{R}^3 \ni x \mapsto \mathcal{S}(x) \in \mathbb{R}^{3\times 3}$ yields a skew-symmetric matrix and it satisfies $\mathcal{S}(a) b := a \times b$, for any $a, b \in \mathbb{R}^3$. $\mathbb{S}^n := \{x \in \mathbb{R}^{n+1} : x^T x = 1\}$ denotes the set of unit vectors in $\mathbb{R}^{n+1}$. The map $\Pi : \mathbb{S}^2 \ni x \mapsto \Pi(x) := I_3 - x x^T \in \mathbb{R}^{3\times 3}$ yields a matrix that represents the orthogonal projection onto the subspace perpendicular to $x \in \mathbb{S}^2$. Denote $d_{\mathbb{R}^n} : \mathbb{R}^n \times \mathbb{R}^n \ni (a, b) \mapsto d_{\mathbb{R}^n}(a, b) := \|a - b\| \in \mathbb{R}_{\geq 0}$ as the standard metric in $\mathbb{R}^n$. Denote $A_1 \oplus \cdots \oplus A_n$ as the block diagonal matrix with block diagonal entries $A_1$ to $A_n$ (square matrices). We denote by $e_1, \cdots, e_n \in \mathbb{R}^n$ the canonical basis vectors in $\mathbb{R}^n$; when clear from the context the Eucledian space the vectors belong to is omitted. For some set $A$, $\mathrm{id}_A : A \ni x \mapsto \mathrm{id}_A(x) := x \in A$ denotes the identity map on that set. Given some normed spaces $A$ and $B$, and a function $f : A \ni a \mapsto f(a) \in B$, $Df : A \ni a \mapsto Df(a) \in \mathcal{L}(A, B)$ denotes the derivative of $f$ ($\mathcal{L}(A, B)$ denotes the set of linear maps from $A$ to $B$). Given a manifold $A$, $T_a A$ denotes the tangent set of $A$ at a point $a \in A$.

## III. RIGID BODY KINEMATICS AND DYNAMICS

The system we model in the next section is composed of two physically coupled rigid bodies. It is thus convenient to present first the notation and preliminaries on a rigid body kinematics and dynamics.

Consider a rigid body with mass $M > 0$ and moment of inertia $J = J^T \in \mathbb{R}^{3\times 3}$ ($J > 0$). A rigid body is described with a pose $P_{\mathbb{SE}} := (P, R) \in \mathbb{SE}(3) := \mathbb{R}^3 \times \mathbb{SO}(3)$, as

a pair composed of a linear position and angular position (orientation); and a twist $V_{\mathbb{SE}} := (V, \Omega) \in \mathbb{R}^3 \times \mathbb{R}^3$, as a pair composed of a linear velocity and an angular velocity (the linear velocity $V$ is expressed in the inertial frame, and the angular velocity $\Omega$ is expressed in the body frame). A rigid body kinematics are then given by (hereafter, you may read the subindex $rb$ as rigid body)

$$K_{rb} : \mathbb{SE}(3) \times \mathbb{R}^6 \ni P_{\mathbb{SE}} \times V_{\mathbb{SE}} \mapsto K_{rb}(P_{\mathbb{SE}}, V_{\mathbb{SE}}) \in T_{P_{\mathbb{SE}}}\mathbb{SE}(3)$$

$$K_{rb}(P_{\mathbb{SE}}, V_{\mathbb{SE}}) := \begin{bmatrix} V \\ R\mathcal{S}(\Omega) \end{bmatrix} \left( = \begin{bmatrix} \dot{P} \\ \dot{R} \end{bmatrix} = \dot{P}_{\mathbb{SE}} \right). \tag{1}$$

Suppose the rigid body is subjected to a wrench $W_{net} := (F_{net}, \tau_{net}) \in \mathbb{R}^3 \times \mathbb{R}^3$ with a net force $F_{net}$ expressed in the inertial frame and a net torque $\tau_{net}$ expressed in the body frame. The rigid body dynamics are then given by

$$D_{rb} : \mathbb{R}^6 \times \mathbb{R}^6 \ni V_{\mathbb{SE}} \times W_{net} \mapsto D_{rb}(V_{\mathbb{SE}}, W_{net}) \in \mathbb{R}^6 \tag{2}$$

$$D_{rb}(V_{\mathbb{SE}}, W_{net}) := \begin{bmatrix} \frac{1}{M}F_{net} \\ J^{-1}(\tau_{net} - \mathcal{S}(\Omega)J\Omega) \end{bmatrix} \left( = \begin{bmatrix} \dot{V} \\ \dot{\Omega} \end{bmatrix} = \dot{V}_{\mathbb{SE}} \right).$$

The linear acceleration equation in (2) comes from the Netwon's equation of motion (the net force determines the time rate of the linear momentum, i.e., $\frac{d}{dt}mV = F_{net}$), while the angular acceleration equation in (2) comes from the Euler's equation of motion (the net torque determines the time rate of the angular momentum, i.e., $\frac{d}{dt}RJ\Omega = R\tau_{net}$).

*Definition 1:* Let $R \in \mathbb{SO}(3)$ be some rotation matrix, and denote

$$R_{\mathbb{SE}} := \begin{bmatrix} I_3 & 0_{3\times3} \\ 0_{3\times3} & R \end{bmatrix} \in \mathbb{R}^{6\times6}. \tag{3}$$

It follows from the definition of the rigid body kinematics in (1) that

$$K_{rb}(P_{\mathbb{SE}}R_{\mathbb{SE}}, R_{\mathbb{SE}}^T V_{\mathbb{SE}}) = K_{rb}(P_{\mathbb{SE}}, V_{\mathbb{SE}})R_{\mathbb{SE}}, \tag{4}$$

for any pose $P_{\mathbb{SE}} \in \mathbb{SE}(3)$, any twist $V_{\mathbb{SE}} \in \mathbb{R}^6$ and any rotation matrix $R \in \mathbb{SO}(3)$. We say that the *rigid body dynamics $D_{rb}$ in (2) are invariant to a rotation $R \in \mathbb{SO}(3)$ ($R \neq I_3$), if*

$$D_{rb}(R_{\mathbb{SE}}^T V_{\mathbb{SE}}, R_{\mathbb{SE}}^T W_{net}) = R_{\mathbb{SE}}^T D_{rb}(V_{\mathbb{SE}}, W_{net}), \tag{5}$$

for any twist $V_{\mathbb{SE}} \in \mathbb{R}^6$, any wrench $W_{net} \in \mathbb{R}^6$ and any rotation matrix $R \in \mathbb{SO}(3)$ (we suppose $R \neq I_3$, otherwise (5) is trivially satisfied).

*Remark 1:* Let us provide some intuition behind the Definition 1. The dynamics relation in (5) can be written as (let $V_{\mathbb{SE}}$ be some function of time)

$$(R_{\mathbb{SE}}^T \dot{V}_{\mathbb{SE}}) = R_{\mathbb{SE}}^T(\dot{V}_{\mathbb{SE}}), \tag{6}$$

which does not hold in general. In fact, (6) only holds if the dynamics (2) are invariant to the rotation $R \in \mathbb{SO}(3)$: if that is the case, the dynamics do not *see* any difference if the rigid body frame is rotated by $R \in \mathbb{SO}(3)$; i.e., if two initial twists are the same up to a rotation ($V_{\mathbb{SE}}^1(0) = R_{\mathbb{SE}}^T V_{\mathbb{SE}}^2(0)$), then the twists evolving according to the dynamics (2) remain the same up to a rotation ($V_{\mathbb{SE}}^1(t) = R_{\mathbb{SE}}^T V_{\mathbb{SE}}^2(t)$ for all $t \geq 0$), regardless of the wrench that is applied on the rigid body.

Similarly, the kinematics relation in (4) can be written as
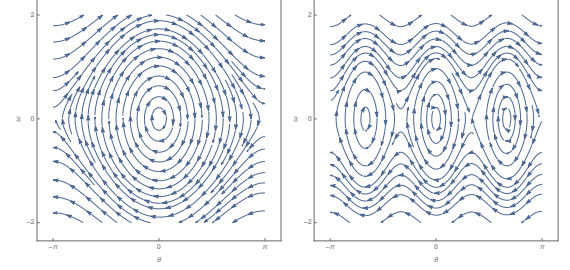


(a) Vector field in $(\theta, \omega) \in [-\pi, \pi] \times [-2, 2]$.
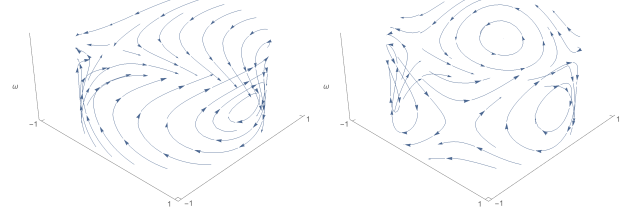


(b) Vector field in cylinder, $\mathbb{S}^2 \times \mathbb{R}$.

Fig. 2: Simple $1D$ rigid body dynamics, with pose $\theta$ and twist $\omega$ (a rotation in this rigid body corresponds to an offset in the pose $\theta$). Left: $(\dot{\theta}, \dot{\omega}) = (\omega, -\sin(\theta))$. Right: $(\dot{\theta}, \dot{\omega}) = (\omega, -\sin(3\theta))$. Left dynamics is not invariant to any rotation, and right dynamics is invariant to $\pm\frac{2\pi}{3} = \pm120°$ rotations.

(let $P_{\mathbb{SE}}$ be some function of time)

$$(P_{\mathbb{SE}}\dot{R}_{\mathbb{SE}}) = (\dot{P}_{\mathbb{SE}})R_{\mathbb{SE}}, \tag{7}$$

which means the kinematics do not *see* any difference if the rigid body frame is rotated: i.e., if two initial poses are the same up to a rotation ($P_{\mathbb{SE}}^1(0) = P_{\mathbb{SE}}^2(0)R_{\mathbb{SE}}$) and the twists are always the same up to a rotation ($V_{\mathbb{SE}}^1(t) = R_{\mathbb{SE}}^T V_{\mathbb{SE}}^2(t)$ for all $t \geq 0$), then the poses evolving according to the kinematics (1) remain the same up to the same rotation ($P_{\mathbb{SE}}^1(t) = P_{\mathbb{SE}}^2(t)R_{\mathbb{SE}}$ for all $t \geq 0$). Fig. 2 exemplifies this concept, with one example dynamics that is not invariant to any rotation, and one example dynamics that is invariant to two (different) rotations.

Since we pose tracking problems in the next section, we introduce here the standard metric in $\mathbb{SE}(3)$, defined as

$$d_{\mathbb{SE}} : \mathbb{SE}(3) \times \mathbb{SE}(3) \ni (P_{\mathbb{SE}}^1, P_{\mathbb{SE}}^2) \mapsto d_{\mathbb{SE}}(P_{\mathbb{SE}}^1, P_{\mathbb{SE}}^2) \in \mathbb{R}_{\geq 0},$$

$$d_{\mathbb{SE}}(P_{\mathbb{SE}}^1, P_{\mathbb{SE}}^2) := \sqrt{\|P^1 - P^2\|^2 + d_{\mathbb{SO}}^2(R^1, R^2)}, \tag{8}$$

$$d_{\mathbb{SO}}^2(R^1, R^2) := 2\text{tr}(I_3 - (R^1)^T R^2),$$

where we emphasize that $d_{\mathbb{SO}}$ is insensitive to rotations of its arguments, i.e.,

$$d_{\mathbb{SO}}^2(R^1, R^2) = d_{\mathbb{SO}}^2(RR^1, RR^2) = d_{\mathbb{SO}}^2(R^1R, R^2R), \tag{9}$$

for any rotation matrices $R, R^1, R^2 \in \mathbb{SO}(3)$.

## IV. Modeling and Problem Statement

Consider the system illustrated in Fig. 3, composed of two rigid bodies, namely one quadrotor (which, for brevity, we refer to as UAV hereafter) and a manipulator (with a load at its end-effector). The two rigid bodies are coupled, with a ball-joint connecting them at the center-of-mass of the UAV. If the ball-joint were absent, the manipulator would behave

(a) Poses of UAV and manipulator, and constraint between rigid bodies.



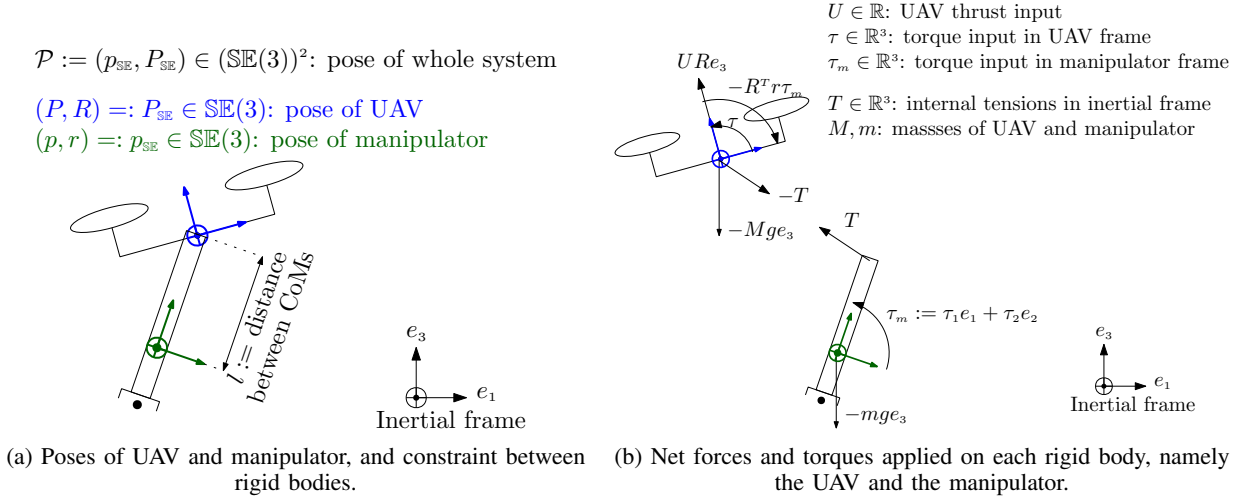(b) Net forces and torques applied on each rigid body, namely the UAV and the manipulator.

Fig. 3: Modeling of coupled UAV and manipulator, the two rigid bodies the system is composed of. Figure 1 provides a screenshot of the real system.

as a free falling (un-actuated) rigid body, while the quadrotor vehicle would behave as a *standard* quadrotor. In its presence, the ball-joint imposes a kinematic constraint, specifically, it enforces the UAV's position to be fixed in the manipulator's orientation frame. This kinematic constraint *links* the UAV and the manipulator, and it provides a way to control the manipulator by means of actuation on the UAV.

For brevity, let us list the physical constants that describe the system (we use upper-case symbols for the UAV's constants, and lower-case symbols for the manipulator's):

- distance between rigid bodies centers-of-mass: $l > 0$.
- quadrotor's mass and moment of inertia: $M > 0$ and $J = J^T \in \mathbb{R}^{3\times3}$;
- manipulator's mass and moment of inertia: $m > 0$ and

$$j := j_{xy} \oplus j_{xy} \oplus j_{zz} = \begin{bmatrix} j_{xy} & 0 & 0 \\ 0 & j_{xy} & 0 \\ 0 & 0 & j_{zz} \end{bmatrix} \in \mathbb{R}^{3\times3}. \quad (10)$$

Let us also list the poses (linear and angular positions) and twists (linear and angular velocities) of the two rigid bodies that compose the system:

- quadrotor's pose – $P_{\mathbb{SE}} \in \mathbb{SE}(3) :\Leftrightarrow (P, R) \in \mathbb{R}^3 \times \mathbb{SO}(3)$;
- manipulator's pose – $p_{\mathbb{SE}} \in \mathbb{SE}(3) :\Leftrightarrow (p, r) \in \mathbb{R}^3 \times \mathbb{SO}(3)$;
- quadrotor's twist – $V_{\mathbb{SE}} \in \mathbb{R}^6 :\Leftrightarrow (V, \Omega) \in \mathbb{R}^3 \times \mathbb{R}^3$;
- manipulator's twist – $v_{\mathbb{SE}} \in \mathbb{R}^6 :\Leftrightarrow (v, \omega) \in \mathbb{R}^3 \times \mathbb{R}^3$.

Finally, let us list the inputs that act on the system, and for which we propose control laws later:

- quadrotor's thrust input – $U \in \mathbb{R}$;
- quadrotor's torque input in the quadrotor's orientation frame – $\tau \in \mathbb{R}^3$;
- manipulator's torque input in the manipulator's orientation frame –

$$\tau_m := \tau_{m,1} e_1 + \tau_{m,2} e_2 \in \mathbb{R}^3. \quad (11)$$

*Remark 2:* The manipulator is taken to be a rod-like rigid body with axial symmetry; as such, rotations of the manipulator around its axis of symmetry may be ignored, which

motivates the absence of a component of the manipulator's torque input along that axis. As illustrated in Fig. 3b, the axis of axial symmetry is the third axis, thus explaining the absence of a torque along the third axis in (11).

For convenience, denote the pose and twist of the system as the pair of poses and twists of the individual rigid bodies, namely,

$$\mathcal{P} \in (\mathbb{SE}(3))^2 :\Leftrightarrow (p_{\mathbb{SE}}, P_{\mathbb{SE}}) \in \mathbb{SE}(3) \times \mathbb{SE}(3), \text{and} \quad (12)$$
$$\mathcal{V} \in (\mathbb{R}^6)^2 :\Leftrightarrow (v_{\mathbb{SE}}, V_{\mathbb{SE}}) \in \mathbb{SE}(3) \times \mathbb{SE}(3). \quad (13)$$

We let our state be composed of the system pose and twist as defined in (12) and (13), and define the state space as

$$\mathbb{X} := \big\{ (\mathcal{P}, \mathcal{V}) \in (\mathbb{SE}(3))^2 \times (\mathbb{R}^6)^2 : \quad (14)$$
$$p + lre_3 - P = 0_3,$$
$$v + lr\mathcal{S}(\omega) e_3 - V = 0_3 \big\},$$

which encapsulates the constraints imposed by the ball-joint, specifically, that the quadrotor's position is fixed w.r.t. the manipulator's orientation frame, i.e., that $r^T(P - p) = le_3 \Leftrightarrow p + lre_3 - P = 0_3$ (recall that $r \in \mathbb{SO}(3)$ represents the manipulator orientation frame). Hereafter, we always decompose a state and an input in the same way, namely

$$x \in \mathbb{X} :\Leftrightarrow (\mathcal{P}, \mathcal{V}) \in \mathbb{X} :\Leftrightarrow (p_{\mathbb{SE}}, P_{\mathbb{SE}}, v_{\mathbb{SE}}, V_{\mathbb{SE}}) \in \mathbb{X} \quad (15)$$
$$:\Leftrightarrow (p, r, P, R, v, \omega, V, \Omega) \in \mathbb{X},$$
$$u \in \mathbb{U} := \mathbb{R}^7 :\Leftrightarrow (U, \tau, \tau_m) \in \mathbb{R} \times \mathbb{R}^3 \times \mathbb{R}^3. \quad (16)$$

Because we are interested in tracking problems for the system just described, we need a metric in the state space $\mathbb{X}$, which is inherited from the metric in $\mathbb{SE}(3)$ in (8); specifically,

$$d_{\mathbb{X}} : \mathbb{X} \times \mathbb{X} \ni (x^1, x^2) \mapsto d_{\mathbb{X}}(x^1, x^2) \in \mathbb{R}_{\geq 0} \quad (17)$$
$$d_{\mathbb{X}}^2(x^1, x^2) := d_{\mathbb{SE}}^2(p_{\mathbb{SE}}^1, p_{\mathbb{SE}}^2) + \|v_{\mathbb{SE}}^1 - v_{\mathbb{SE}}^2\|^2 +$$
$$d_{\mathbb{SE}}^2(P_{\mathbb{SE}}^1, P_{\mathbb{SE}}^2) + \|V_{\mathbb{SE}}^1 - V_{\mathbb{SE}}^2\|^2.$$

Given the state space definition in (14), one may compute its tangent set at any point $x \in \mathbb{X}$ (see state decomposition

in (15)), which is given by

$$T_x\mathbb{X} := \left\{ (\delta\mathcal{P}, \delta\mathcal{V}) \in T_{\mathcal{P}}(\mathbb{SE}(3))^2 \times (\mathbb{R}^6)^2 : \right. \tag{18}$$
$$\delta p + l\delta r e_3 - \delta P = 0_3,$$
$$\left. \delta v + l\delta r \mathcal{S}(\omega) e_3 + l r \mathcal{S}(\delta\omega) e_3 - \delta V = 0_3 \right\},$$

which is critical in computing the internal forces that allow the restrictions in (14) to be satisfied.

Given an appropriate input $u : \mathbb{R}_{\geq 0} \ni t \mapsto u(t) \in \mathbb{U}$, a system's trajectory $x : \mathbb{R}_{\geq 0} \ni t \mapsto x(t) \in \mathbb{X}$ evolves according to

$$\dot{x}(t) = X(x(t), u(t)), x(0) \in \mathbb{X}, \tag{19}$$

where the vector field $X$ is given by

$$X : \mathbb{X} \times \mathbb{U} \ni (x, u) \mapsto X(x, u) \in T_x\mathbb{X}$$
$$X(x, u) := \begin{bmatrix} K_X(\mathcal{P}, \mathcal{V}) \\ D_X(x, u) \end{bmatrix} \left( = \begin{bmatrix} \dot{\mathcal{P}} \\ \dot{\mathcal{V}} \end{bmatrix} = \begin{bmatrix} \text{kinematics} \\ \text{dynamics} \end{bmatrix} \right), \tag{20}$$

where the kinematics $K_X$ are given by (recall the rigid body kinematics $K_{rb}$ in (1))

$$K_X(\mathcal{P}, \mathcal{V}) := \begin{bmatrix} K_{rb}(p_{\mathbb{SE}}, v_{\mathbb{SE}}) \\ K_{rb}(P_{\mathbb{SE}}, V_{\mathbb{SE}}) \end{bmatrix} \left( = \begin{bmatrix} \dot{p}_{\mathbb{SE}} \\ \dot{P}_{\mathbb{SE}} \end{bmatrix} \right) \tag{21}$$

$$= \begin{bmatrix} v \\ \dfrac{r\mathcal{S}(\omega)}{V} \\ R\mathcal{S}(\Omega) \end{bmatrix} \left( = \begin{bmatrix} \dot{p} \\ \dot{r} \\ \dot{P} \\ \dot{R} \end{bmatrix} \right), \tag{22}$$

and the dynamics $D_X$ are given by (recall the rigid body dynamics $D_{rb}$ in (2))

$$D_X(x, u) := \begin{bmatrix} D_{rb}(v_{\mathbb{SE}}, W_{net}^{man}) \\ D_{rb}(V_{\mathbb{SE}}, W_{net}^{uav}) \end{bmatrix} \left( = \begin{bmatrix} \dot{v}_{\mathbb{SE}} \\ \dot{V}_{\mathbb{SE}} \end{bmatrix} \right), \tag{23}$$

$$W_{net}^{man} \equiv \begin{bmatrix} F_{net}^{man} \\ \tau_{net}^{man} \end{bmatrix} \equiv \begin{bmatrix} T(x, u) - mge_3 \\ \tau_m + l\mathcal{S}(e_3) r^T T(x, u) \end{bmatrix}, \tag{24}$$

$$W_{net}^{uav} \equiv \begin{bmatrix} F_{net}^{uav} \\ \tau_{net}^{uav} \end{bmatrix} \equiv \begin{bmatrix} URe_3 - T(x, u) - Mge_3 \\ \tau - R^T r\tau_m \end{bmatrix}, \tag{25}$$

with $g$ as the acceleration due to gravity and where the internal tension forces $T(x, u)$ (expressed in the inertial frame) are given by (26). (We emphasize the introduction of the adimensional constant $\gamma$ in (27); we introduce it for convenience, and, at this point, we only emphasize that $\gamma = 1$ when the manipulator is taken as a point-mass.) The analytic expression of the wrenches (pair net force and net torque) in (24) and (25) applied on the manipulator and the UAV is deduced by inspection of Fig. 3b. The system dynamics in (23) can be written equivalently as

$$D_X(x, u) = \tag{28}$$
$$= \begin{bmatrix} \frac{1}{m}(T(x, u) - mge_3) \\ j^{-1}(\tau_m + l\mathcal{S}(e_3) r^T T(x, u) - \mathcal{S}(\omega) j\omega) \\ \frac{1}{M}(URe_3 - T(x, u) - Mge_3) \\ J^{-1}(\tau - R^T r\tau_m - \mathcal{S}(\Omega) J\Omega) \end{bmatrix} \left( = \begin{bmatrix} \dot{v} \\ \dot{\omega} \\ \dot{V} \\ \dot{\Omega} \end{bmatrix} \right)$$
$$\overset{(11)}{\underset{(10)}{=}} \begin{bmatrix} \frac{1}{m}(T(x, u) - mge_3) \\ \frac{\tau_m}{j_{xy}} + \frac{l}{j_{xy}}\mathcal{S}(e_3) r^T T(x, u) + \left( \frac{j_{zz}}{j_{xy}} - 1 \right) e_3^T \omega \mathcal{S}(e_3)\omega \\ \frac{1}{M}(URe_3 - T(x, u) - Mge_3) \\ J^{-1}(\tau - R^T r\tau_m - \mathcal{S}(\Omega) J\Omega) \end{bmatrix}.$$

The vector field $X$ in (20) is composed of the system kinematics and dynamics. The system kinematics are given by the kinematics of each individual rigid body, in this particular case of the UAV and of the manipulator. On the other hand, the system dynamics are given by the linear and angular accelerations of each individual rigid body, by considering the net force (expressed in the inertial frame) and the net torque (expressed in the respective body frame) applied on each rigid body. The forces and torques contributing to the net force and net torque of each rigid body are visualized in Fig. 3b. It may be useful to discuss the net wrenches applied to each rigid body:

- The tension forces ($T(x, u) \in \mathbb{R}^3$ in (26), expressed in the inertial frame) are internal forces, forming an action-reaction pair, and thus explaining its positive contribution to the manipulator's linear acceleration and its negative contribution to the UAV's.
- The manipulator input torque ($\tau_m \in \mathbb{R}^3$ in (11), expressed in the manipulator frame) also forms an action-reaction pair, thus explaining its positive contribution to the manipulator's angular acceleration and its negative contribution to the UAV's (in the UAV's orientation frame, the manipulator input torque is given by $-R^T r\tau_m$).
- The reaction forces to the rigid body weights are applied on the earth, and are thus ignored in our modeling.
- The reaction force and reaction torque to the quadrotor's thrust input ($URe_3$) and torque input ($\tau$) are applied on the air and on the motor propellers, and are thus ignored in our modeling.

The tension forces ($T(x, u) \in \mathbb{R}^3$) constitute internal forces to the system, and the Newton's and Euler's equations of motion do not provide any insight into these forces. However, the constraint that the state must remain in the state set $\mathbb{X}$ in (14), enforces the vector field $X$ in (20) to be in the tangent set of that set. This constraint uniquely defines the tensions, i.e., for any $(x, u) \in \mathbb{X} \times \mathbb{U}$,

$$X(x, u) \in T_x\mathbb{X} \Rightarrow T(x, u) \text{ as in (26)}. \tag{29}$$

The Euler-Lagrange formalism provides an alternative, but equivalent, approach for obtaining the vector field in (20).

*Proposition 3:* The rotation of the manipulator around its axis of axial symmetry (third axis) is constant, i.e., along a solution $t \to x(t) \in \mathbb{X}$ of (19), $t \to e_3^T \omega(t) = e_3^T \omega(0) \in \mathbb{R}$.

*Proof 1:* For convenience, define the function $f : \mathbb{X} \ni x \mapsto f(x) := e_3^T \omega \in \mathbb{R}$. It follows that, for any $(x, u) \in \mathbb{X} \times \mathbb{U}$, $Df(x)X(x, u) = e_6^T D_X(x, u) = e_3^T j^{-1}(\tau_m + l\mathcal{S}(e_3) T(x, u) - \mathcal{S}(\omega) j\omega) \overset{(10),(11)}{=} 0$, which concludes the proof.

Proposition 3 implies that the rotation of the manipulator around its axis of symmetry, despite uncontrollable, remains constant along solutions. One could, at this point, assume that the rotation around that axis is non-existing at the initial time instant; however, we shall make that assumption only in one of the problems treated in this manuscript (for the UAV-slung-manipulator system, that we describe next).

*Proposition 4:* Recall Definition 1 and assume that the

$$T : \mathbb{X} \times \mathbb{U} \ni (x, u) \mapsto T(x, u) \in \mathbb{R}^3 \tag{26}$$

$$T(x, u) := r \left( \left( \frac{1}{m} + \frac{1}{M} \right) I_3 + \frac{l^2}{j_{xy}} \Pi(e_3) \right)^{-1} \left( \frac{U}{M} r^T R e_3 + \frac{l}{j_{xy}} \mathcal{S}(e_3) \tau_m + l \left( \omega^T \Pi(e_3) \omega e_3 - \frac{j_{zz}}{j_{xy}} e_3^T \omega \Pi(e_3) \omega \right) \right)$$

$$= \frac{1}{\gamma} r \left( \left( \frac{j_{xy}}{l^2} I_3 + \frac{mM}{m + M} e_3 e_3^T \right) \left( \frac{U}{M} r^T R e_3 + l \omega^T \Pi(e_3) \omega e_3 \right) + \frac{1}{l} \left( \mathcal{S}(e_3) \tau_m - j_{zz} e_3^T \omega \Pi(e_3) \omega \right) \right)$$

$$\gamma \equiv 1 + \frac{j_{xy}}{l^2} \frac{m + M}{mM} \tag{27}$$

moment of inertia of the UAV is given as

$$J = J_{xy} \oplus J_{xy} \oplus J_{zz} = \begin{bmatrix} J_{xy} & 0 & 0 \\ 0 & J_{xy} & 0 \\ 0 & 0 & J_{zz} \end{bmatrix} \in \mathbb{R}^{3 \times 3}. \tag{30}$$

Then, the vector field $X$ in (20) is invariant to rotations of the manipulator around its third axis (the axis of axial symmetry) and to rotations of the UAV around its third axis (the thrust axis).

*Proof 2:* Define

$$R_z : \mathbb{R} \ni \theta \mapsto R_z(\theta) \in \mathbb{SO}(3)$$

$$R_z(\theta) := \begin{bmatrix} \cos(\theta) & -\sin(\theta) & 0 \\ \sin(\theta) & \cos(\theta) & 0 \\ 0 & 0 & 1 \end{bmatrix}, \tag{31}$$

as a rotation matrix around the third axis. Pick a $\theta_p \in \mathbb{R}$ and a $\theta_P \in \mathbb{R}$, and define for convenience (recall the notation introduced in (3))

$$R = (R_z(\theta_p))_{\mathbb{SE}} \oplus (R_z(\theta_P))_{\mathbb{SE}}$$

$$= \begin{bmatrix} (R_z(\theta_p))_{\mathbb{SE}} & 0_{6 \times 6} \\ 0_{6 \times 6} & (R_z(\theta_P))_{\mathbb{SE}} \end{bmatrix} \in \mathbb{R}^{12 \times 12}. \tag{32}$$

It follows that, given a system pose $\mathcal{P} := (p, r, P, R) \in (\mathbb{SE}(3))^2$,

$$\mathcal{P}R \stackrel{(12)}{=} \begin{bmatrix} p \\ r R_z(\theta_p) \\ P \\ R R_z(\theta_P) \end{bmatrix} \in (\mathbb{SE}(3))^2, \tag{33}$$

thus corresponding to a rotation of the manipulator around its third axis (by an angle $\theta_p$) and to a rotation of the UAV around its third axis (by an angle $\theta_P$). It also follows that, given a system twist $\mathcal{V} := (v, \omega, V, \Omega) \in (\mathbb{R}^3)^4$,

$$R^T \mathcal{V} \stackrel{(13)}{=} \begin{bmatrix} v \\ R_z^T(\theta_p) \omega \\ V \\ R_z^T(\theta_P) \Omega \end{bmatrix} \in (\mathbb{R}^3)^4, \tag{34}$$

thus corresponding to the twist of the system (the angular velocities are expressed in the body frame's of their respective rigid body) when the rigid bodies are rotated around their third axes. It is straightforward to verify that

$$D_X((\mathcal{P}R, R^T \mathcal{V}), (U, R_z^T(\theta_P) \tau, R_z^T(\theta_p) \tau_m)) =$$
$$= R D_X((\mathcal{P}, \mathcal{V}), (U, \tau, \tau_m)), \tag{35}$$

for any pair pose and twist $(\mathcal{P}, \mathcal{V}) \stackrel{(14)}{\in} \mathbb{X}$ and any input $(U, \tau, \tau_m) \in \mathbb{R}^7$ with $\tau_m$ as in (11) (vectors in the manipulator frame must be rotated by $R_z^T(\theta_p)$, while vectors in the UAV

frame must be rotated by $R_z^T(\theta_P)$). (For brevity, let us verify (35) by checking only one term, namely $J^{-1} R r^T \tau_m$ in the UAV's angular acceleration $\dot{\Omega}$: indeed $R_z(\theta_P)^T J^{-1} R^T r \tau_m = R_z(\theta_P)^T J^{-1} R_z(\theta_P)(R R_z(\theta_P))^T (r R_z(\theta_P))(R_z(\theta_P)^T \tau_m)$, and where one can verify that $R_z(\theta_P)^T J^{-1} R_z(\theta_P) = J^{-1}$ is independent of $\theta_P$, provided that $J$ is as in (30). Complete verification of (35) follows similar steps as those just described).

*Remark 5:* Proposition 4 only holds if the UAV moment of inertia has the form shown in (30), where the moments of inertia along the first and second axes are the same. This assumption is lifted if the UAV input torque is chosen such that the UAV behaves as if it has a unitary moment of inertia (i.e., if $\tau = J \tau' + R^T r \tau_m + \mathcal{S}(\Omega) J \Omega$ then $\dot{\Omega} = \tau'$), which is precisely the approach we take later in this manuscript.

Proposition 4 implies that the dynamics do not see rotations of the rigid bodies around their third axes (see Remark 1). This motivates us to control the space orthogonal to the manipulator's third axis and the UAV's third axis as separate problems. Loosely speaking, we can treat the yaw position of the manipulator and of the UAV as separate problems: the yaw motion of the UAV can be understood from $R e_1$, $R e_2$ and $e_3^T \Omega$; similarly, the yaw motion of the manipulator can be understood from $r e_1$, $r e_2$ and $e_3^T \omega$ (and we shall ignore this motion since $e_3^T \omega$ is uncontrollable – see Proposition 3).

Invariance to rotations around the third axes also motivates us to introduce an equivalence relation in the set $\mathbb{X}$ in (14). To be specific, consider two states in $\mathbb{X}$, namely $x_1 = (\mathcal{P}_1, \mathcal{V}_1) \in \mathbb{X}$ and $x_2 = (\mathcal{P}_2, \mathcal{V}_2) \in \mathbb{X}$; then we define the relation $\sim$ as

$$x_1 \sim x_2 :\Leftrightarrow \begin{bmatrix} p_1 \\ r_1 \\ P_1 \\ R_1 \end{bmatrix} = \begin{bmatrix} p_2 \\ r_2 R_z(\theta_p) \\ P_2 \\ R_2 R_z(\theta_p) \end{bmatrix} \text{ and} \tag{36}$$

$$\begin{bmatrix} v_1 \\ \omega_1 \\ V_1 \\ \Omega_1 \end{bmatrix} = \begin{bmatrix} v_2 \\ R_z^T(\theta_p)(\omega_2 + b e_3) \\ V_2 \\ R_z^T(\theta_P)(\Omega_2 + B e_3) \end{bmatrix},$$

for some real $\theta_p$, $\theta_P$, $b$ and $B$; i.e., two states are equivalent up to rotations around their third axes and up to the third component of their body-frame angular-velocities. One can verify that the relation (36) is reflexive, symmetric and transitive, which supports the following result.

*Proposition 6:* The relation defined in (36) is an equivalence relation in $\mathbb{X}$.

Proposition (6) guarantees that one may consider the quotient space induced by the equivalence relation $\sim$ in (36), namely

$$\mathbb{X} \backslash_{\sim} := \{ [x] : x \in \mathbb{X} \}, \tag{37}$$

where $[x] := \{x' \in \mathbb{X} : x' \sim x\}$ denotes the equivalence class associated to some $x \in \mathbb{X}$. We will require the quotient set later, which is the reason why we introduce it at this point. Also, since the metric in $\mathbb{SO}(3)$ is insensitive to rotation of its arguments – see (9) – it follows that the quotient set $\mathbb{X}\backslash_\sim$ can inherit the metric $d_\mathbb{X}$ as defined in (17), leading to the definition

$$d_{\mathbb{X}\backslash_\sim} : \mathbb{X}\backslash_\sim \times \mathbb{X}\backslash_\sim \ni ([x^1], [x^2]) \mapsto d_{\mathbb{X}\backslash_\sim}([x^1], [x^2]) \in \mathbb{R}_{\geq 0}$$
$$d_{\mathbb{X}\backslash_\sim}([x^1], [x^2]) := d_\mathbb{X}(x^1, x^2). \qquad (38)$$

*Proposition 7:* The metric $d_{\mathbb{X}\backslash_\sim}$ in (38) is well-defined.

*Proof 3:* The metric $d_{\mathbb{X}\backslash_\sim}$ in (38) is defined with respect to representatives of an equivalence class, so we must show that that definition yields the same result regardless of the choice of representatives. (Since the metric is symmetric, it suffices to check independence of choice of representative for the first entry of the metric.) For that purpose, let $x \in \mathbb{X}$ and consider the equivalence class $[x] \in \mathbb{X}\backslash_\sim$. Consider then two distinct elements of that class, namely $\tilde{x} \in [x]$ and $\bar{x} \in [x]$, where $\tilde{x} \neq \tilde{x}$. Since those states are equivalent, i.e., $\tilde{x} \sim \bar{x}$, it follows from the definition of the equivalence relation in (36) that $(\tilde{p}, \tilde{r}, \tilde{P}, \tilde{R}, \tilde{v}, \tilde{\omega}, \tilde{V}, \tilde{\Omega}) = (\bar{p}, \bar{r}R_z(\theta_p), \bar{P}, \bar{R}R_z(\theta_P), \bar{v}, R_z^T(\theta_p)(\bar{\omega} + be_3), \bar{V}, R_z^T(\theta_P)(\bar{\Omega} + Be_3))$, for some real $\theta_p, \theta_P, b$ and $B$. Finally, consider another $x^\star \in \mathbb{X}$. It follows that

$$d_{\mathbb{X}\backslash_\sim}^2([\tilde{x}], [x^\star]) \overset{(38)}{=} d_\mathbb{X}^2(\tilde{x}, x^\star)$$
$$\overset{(17)}{=} \ldots + d_{\mathbb{SO}}^2(\tilde{R}, R^\star) + \|\tilde{\Omega} - \Omega^\star\|^2$$
$$\overset{(\tilde{x}\sim\bar{x})}{=} \ldots + d_{\mathbb{SO}}^2(\bar{R}R_z(\theta_P), R^\star) + \|R_z^T(\theta_P)(\bar{\Omega} + Be_3) - \Omega^\star\|^2$$
$$\overset{(9)}{=} \ldots + d_{\mathbb{SO}}^2(\bar{R}, R^\star R_z^T(\theta_P)) + \|\bar{\Omega} - R_z(\theta_P)(\Omega^\star - Be_3)\|^2$$
$$\overset{(17)}{=} d_\mathbb{X}^2(\bar{x}, \bar{x}^\star), \text{ where } \bar{x}^\star \sim x^\star$$
$$\overset{(38)}{=} d_{\mathbb{X}\backslash_\sim}^2([\bar{x}], [\bar{x}^\star]) \overset{\bar{x}^\star \sim x^\star}{=} d_{\mathbb{X}\backslash_\sim}^2([\bar{x}], [x^\star]),$$

which completes the proof.

We consider two separate problems – see Fig. 4 – on the system just described: in the first we consider the manipulator torque input in (11) to be available, while in the second we restrict that torque input to be zero.

### A. UAV-manipulator system

Hereafter, we refer to *UAV-manipulator system* when considering the manipulator torque input in (11) is available. With Fig. 4a in mind, we can then formulate the first problem treated in this paper, which is one of semi-pose tracking: we require the manipulator's position to track a desired position trajectory, and the manipulator axis of axial symmetry ($re_3$ in our case) to track a desired attitude trajectory. The space orthogonal to the manipulator axis is ignored, for the reasons discussed after Proposition 3 (and thus the semi-pose tracking rather than (full-)pose tracking).
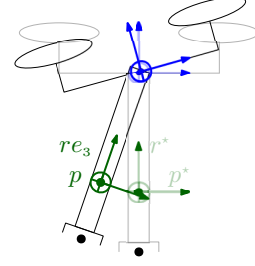
*Problem 1 (UAV-Manipulator):* Consider the vector field $X$ in (20). Given a desired position trajectory and a desired orientation trajectory, i.e,

$$p^\star : \mathbb{R}_{\geq 0} \ni t \mapsto p^\star(t) \in \mathbb{R}^3, \qquad (39)$$
$$r^\star : \mathbb{R}_{\geq 0} \ni t \mapsto r^\star(t) \in \mathbb{S}^2, \qquad (40)$$
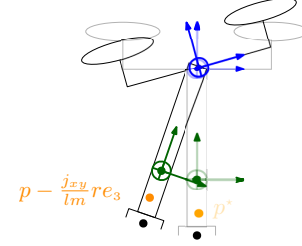


(a) Semi-pose tracking problem for *UAV-manipulator system*: desired semi-pose trajectory $(p^\star, r^\star)$ determines the whole state equilibrium in transparent; i.e., the system is differentially flat w.r.t. $(p, re_3)$.



(b) Position tracking problem for *UAV-slung-manipulator system*: desired position trajectory $p^\star$ determines the whole state equilibrium in transparent; i.e., the system is differentially flat w.r.t. $p - \frac{j_{xy}}{lm}re_3$.

Fig. 4: Two problems: one where the manipulator torque $\tau_m$ is available – Fig. 4a; and one where it is not – Fig. 4b.

design a control law

$$u^{cl} := (U^{cl}, \tau^{cl}, \tau_m^{cl}) : \mathbb{R}_{\geq 0} \times \mathbb{X} \mapsto \mathbb{U}, \qquad (41)$$

such that $\lim_{t\to\infty}(p(t) - p^\star(t)) = 0_3$ and $\lim_{t\to\infty}(re_3 - r^\star(t)) = 0_3$ along the solution $\mathbb{R}_{\geq 0} \ni t \mapsto x(t) \in \mathbb{X}$ of $\dot{x}(t) = X(x(t), u^{cl}(t, x(t)))$ with $x(0) \in \mathbb{X}_0$ for some non-empty $\mathbb{X}_0 \subset \mathbb{X}$.

*Remark 8:* The problem treated here is a generalization of that treated in [47]. In [47], the manipulator is treated as a point-mass and only the kinematics of the quadrotor's attitude are considered. The vector field presented there is in fact recovered as follows:

- Since the constraints in (14) must be satisfied, one imposes that $re_3 = \frac{P-p}{l}$ and that $r\omega = \mathcal{S}\left(\frac{P-p}{l}\right)\frac{V-v}{l}$.
- Since the manipulator is taken as a point mass (and thus has no angular position and angular velocity, i.e., $r$ and $\omega$), the manipulator attitude equations ($\dot{r}$ in (22), and $\dot{\omega}$ in (28)) are ignored.
- Finally, the internal forces are found by taking the limit when the moment of inertia of the manipulator vanishes, i.e., when $j \to 0_{3\times 3} \overset{(10)}{\Leftrightarrow} (j_{xy}, j_{zz}) \to (0, 0)$, leading to (below, $re_3$ and $r\omega$ are those presented above)

$$\lim_{j \to 0_{3\times 3}} T(x, u) \overset{(26)}{=} \frac{m}{m + M}\left(U(re_3)^T Re_3 + lM\|r\omega\|^2\right)re_3 + \frac{1}{l}\mathcal{S}(re_3)r\tau_m.$$

## B. UAV-slung-manipulator system

Hereafter, we refer to *UAV-slung-manipulator system* when considering that the manipulator torque input in (11) is not available (Remark 9 sheds some light into the name *UAV-slung-manipulator system*). With some abuse of notation, and without hindering comprehension, when referring to the UAV-slung-manipulator system, we reuse and redefine the input $u$ and the vector field $X$; to be specific, instead of the input in (16), we redefine it as

$$u = (U, \tau) \in \mathbb{R} \times \mathbb{R}^3, \tag{42}$$

and, instead of the vector field in (20), we redefine it as

$$X : \mathbb{X} \times \mathbb{R}^4 \ni (x, u) \mapsto X(x, u) \in T_x\mathbb{X}$$
$$X(x, u) := X(x, (U, \tau, 0_3))|_{X \text{ in } (20)}. \tag{43}$$

With Fig. 4b in mind, we can then formulate the second problem treated in this paper, which is one of position tracking: we require a specific point along the manipulator's axis of axial symmetry to track a desired position trajectory.

*Problem 2 (UAV-slung-manipulator):* Consider the vector field $X$ in (43). Given a desired position trajectory, i.e,

$$p^\star : \mathbb{R}_{\geq 0} \ni t \mapsto p^\star(t) \in \mathbb{R}^3, \tag{44}$$

design a control law

$$u^{cl} := (U^{cl}, \tau^{cl}) : \mathbb{R}_{\geq 0} \times \mathbb{X} \mapsto \mathbb{R}^4 \tag{45}$$

such that $\lim_{t \to \infty}(p(t) - \frac{j_{xy}}{lm}r(t)e_3 - p^\star(t)) = 0_3$ along a solution $\mathbb{R}_{\geq 0} \ni t \mapsto x(t) \in \mathbb{X}$ of $\dot{x}(t) = X(x(t), u^{cl}(t, x(t)))$ with $x(0) \in \mathbb{X}_0$ for some non-empty $\mathbb{X}_0 \subset \mathbb{X}$.

*Remark 9:* The problem treated here is a generalization of that treated in [48], which deals with the slung-load problem. In [48], the UAV is tethered to a point mass, which is the system here described if we take the manipulator to be a point-mass. The vector field presented there is in fact recovered following the exact same procedure as in Remark 8.

*Remark 10:* In Problem 2, rather than requiring the manipulator's position $p$ to track the desired trajectory, we require another position along the manipulator's axis of symmetry $(p - \frac{j_{xy}}{lm}re_3)$ to track the desired trajectory (note however that those positions coincide when the manipulator is taken as a point mass, i.e., when $j_{xy} = 0$). Let us motivate here why. In a UAV-slung-load problem, requiring the UAV to track a desired trajectory is an ill-defined problem, because the system is differentially flat with respect to the load position, but not with respect to the UAV position: in other words, if the UAV tracks a certain trajectory, the trajectory the load tracks depends on the initial condition. Similarly, in the UAV-slung-manipulator problem, requiring the manipulator (center-of-mass) to track a desired trajectory is an ill-defined problem, because the system is not differentially flat with respect to the manipulator's center-of-mass: rather it is differentially flat with respect to another point (to be specific, $p - \frac{j_{xy}}{lm}re_3$).

*Remark 11:* Notice that Problem 1 describes a semi-pose tracking problem, while Problem 2 describes a position tracking problem. This difference stems from the fact that the UAV-slung-manipulator system is deprived of the manipulator torque input, which prevents the manipulator pose from tracking an arbitrary pose. In fact, as we verify later, for the UAV-slung-manipulator system, the desired position trajectory in (44) imposes a desired semi-pose trajectory (this is verified by means of differential flatness).

## V. CONTROL STRATEGY SUMMARY

In this section, we explain the pursued control strategy, illustrated in Fig. 5. The strategy is composed of three steps, which we explain next. The specifics of these three steps are different when solving Problems 1 and 2, but the overall idea behind them is the same.

Recall then Proposition 4, which states that rotations around the rigid bodies' third axes may be ignored. Our first step is to design a bijective mapping (the specific mapping $f$ and the codomain $\mathbb{Y}$ are specific to each Problem 1 and 2, and are provided later)

$$f : \mathbb{X}\backslash_\sim \ni [x] \mapsto f([x]) =: y \in \mathbb{Y} \tag{46}$$

which reorders the state in a manner that highlights the hierarchical/cascaded structure of the problem, while ignoring the rotations around the rigid bodies third axes: the necessity of the equivalence relation $\sim$ in (36) and of the quotient set $\mathbb{X}\backslash_\sim$ in (37) becomes clear at this point. This step is called state transformation – see Figure 5.

In our second step, we design a control law

$$\bar{u}^{cl} : \mathbb{X} \times \mathbb{U} \times \mathbb{R} \ni (x, v, \tau_\psi) \mapsto \bar{u}^{cl}(x, v, \tau_\psi) \in \mathbb{U} \tag{47}$$

which transforms the input (from $v$ to $u$ – see input transformation in Fig. 5), in such a way that when we compose this input transformation and state transformation with the system dynamics, we obtain the transformed dynamics in $\mathbb{Y}$, i.e.,

$$Y : \mathbb{Y} \times \mathbb{U} \ni (y, v) \mapsto Y(y, v) \in T_y\mathbb{Y} \tag{48}$$
$$Y(y, v) := Df([x])X(x, \bar{u}^{cl}(x, v, \tau_\psi))|_{x \in f^{-1}(y)}(= \dot{y}),$$

where we emphasize that $f^{-1}$ exists since the map $f$ is invertible. Let us emphasize some key points regarding the input transformation $\bar{u}^{cl}$ in (47) and the vector field $Y$ in (48):

- The input transformation $\bar{u}^{cl}$ is designed so as to make make explicit the cascaded structure of the vector field $Y$ (one may think of a chain of integrators);
- The vector field $Y$ is independent of $\tau_\psi \in \mathbb{R}$, which is used to control the space orthogonal to the UAV's third axis (the yaw motion of the UAV, loosely speaking), but not to control the transformed state $y$ in (46) (the transformed state does not *see* rotations around the rigid bodies third axes since $f$ maps from the quotient set $\mathbb{X}\backslash_\sim$);
- We (must) show that the vector field $Y$ in (48) is well defined, in the sense that (48) is independent of the choice of the representative belonging the equivalence class $f^{-1}(y)$ (notice that for any $y \in \mathbb{Y}$, $f^{-1}(y)$ is an equivalence class, i.e., $f^{-1}(y) \in \mathbb{X}\backslash_\sim$).

In the third and final step, we analyze differential flatness properties of the vector field $Y$, and based on that determine the equilibrium (more precisely the equilibria)

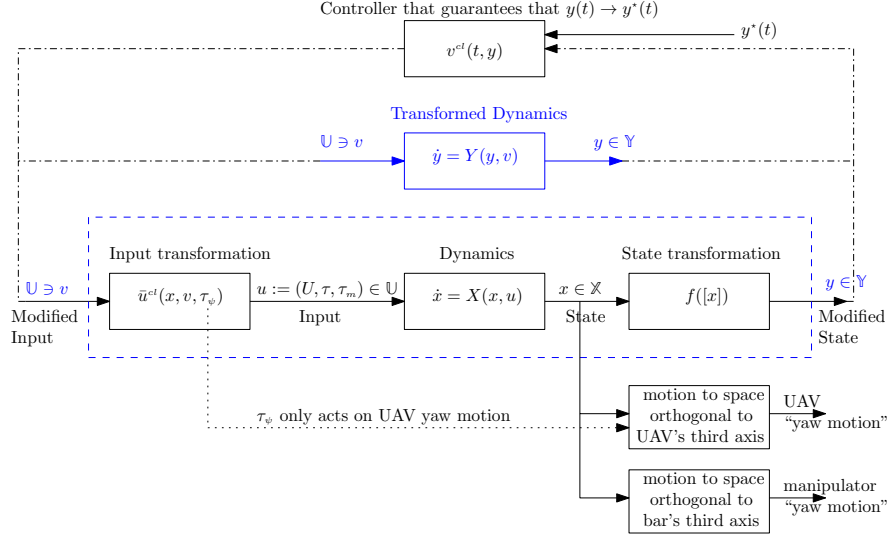$$y^\star : \mathbb{R} \ni t \mapsto y^\star(t) \in \mathbb{Y} \tag{49}$$

Fig. 5: Control strategy block-diagram.

for which it is guaranteed that Problems 1 and 2 are satisfied. Finally, we design a control law

$$v^{cl} : \mathbb{R} \times \mathbb{Y} \ni (t, y) \mapsto v^{cl}(t, y) \in \mathbb{U} \qquad (50)$$

that guarantees that a solution $t \mapsto y(t)$, of $\dot{y}(t) = Y(y(t), v^{cl}(t, y(t)))$, tracks the desired equilibrium $t \mapsto y^{\star}(t)$. Problems 1 and 2 are then accomplished if one composes the input transformation $\bar{u}^{cl}$ in (47) with the control law $v^{cl}$ in (50), i.e.,

$$u^{cl} : \mathbb{R} \times \mathbb{X} \ni (t, x) \mapsto u^{cl}(t, x) \in \mathbb{U}$$
$$u^{cl}(t, x) := \bar{u}^{cl}(x, v^{cl}(t, f([x])), \tau_{\psi}^{cl}(t, x)), \qquad (51)$$

where $\tau_{\psi}^{cl} : \mathbb{R} \times \mathbb{X} \ni (t, x) \mapsto \tau_{\psi}^{cl}(t, x) \in \mathbb{R}$ is some control law designed to control the yaw motion of the UAV (see Fig 5). Let us now look at each Problem individually.

*Remark 12:* Suppose $f : \mathbb{X} \ni x \to f(x) \in \mathbb{Y}$, instead of that in (46), i.e. that $f$ provides a bijective map from $\mathbb{X}$ to $\mathbb{Y}$, or, in other words, a coordinate change from $\mathbb{X}$ to $\mathbb{Y}$. Then, equation (48) would be instead

$$Y(y, v) := Df(x)X(x, \bar{u}^{cl}(x, v, \tau_{\psi}))|_{x = f^{-1}(y)} (= \dot{y}),$$

which is the standard equation for computing the vector field in the new coordinate system in $\mathbb{Y}$.

## VI. UAV-MANIPULATOR PROBLEM

We verify next that the UAV-manipulator system behaves as two decoupled systems, as illustrated in Fig. 6: one thrust-propelled system by considering the motion of the center-of-mass of the whole system (at this point point, the internal forces – $T(x, u)$ – do not play a role); and one unit vector double integrator system corresponding to the attitude dynamics of the manipulator. The three steps we follow next have been described in the previous section.
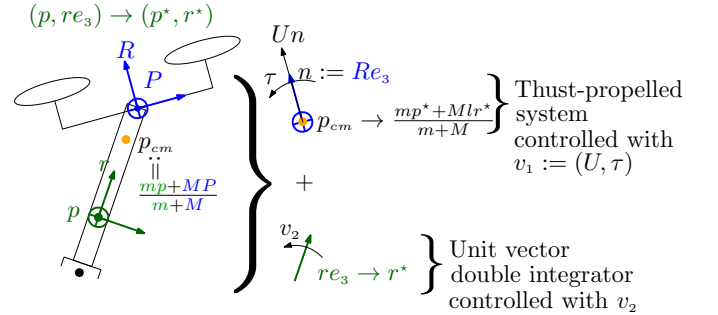


Fig. 6: By means of appropriate state and input transformations, the UAV-manipulator may be understood as two decoupled systems: one thrust-propelled system and one unit-vector double-integrator system.

### A. State transformation

Recall the discussion from Section V Let us then introduce the set $\mathbb{Y}$ as

$$\mathbb{Y} = \mathbb{Y}_1 \times \mathbb{Y}_2 \qquad (52a)$$
$$\mathbb{Y}_1 := \{(p_{cm}, v_{cm}, n, \varpi) \in (\mathbb{R}^3)^4 : n^T n = 1, n^T \varpi = 0\}, \qquad (52b)$$
$$\mathbb{Y}_2 := \{(r, \omega) \in (\mathbb{R}^3)^2 : r^T r = 1, r^T \omega = 0\}, \qquad (52c)$$

with the inherited metrics $d_{\mathbb{Y}_1} := d_{\mathbb{R}^{12}}$, $d_{\mathbb{Y}_2} := d_{\mathbb{R}^6}$ and $d_{\mathbb{Y}} := d_{\mathbb{R}^{18}}$. The set $\mathbb{Y}_1$ will be used for the subsystem that behaves as a thrust-propelled system; while the set $\mathbb{Y}_2$ will be used for the subsystem that behaves as a unit vector double integrator system (see Fig. 6). Hereafter, and for convenience, we decompose elements in the sets above as

$$y \in \mathbb{Y} :\Leftrightarrow (y_1, y_2) \in \mathbb{Y}_1 \times \mathbb{Y}_2, \qquad (53a)$$
$$y_1 \in \mathbb{Y}_1 :\Leftrightarrow (p_{cm}, v_{cm}, n, \varpi) \in \mathbb{Y}_1, \qquad (53b)$$
$$y_2 \in \mathbb{Y}_2 :\Leftrightarrow (r, \omega) \in \mathbb{Y}_2. \qquad (53c)$$

Hereafter, we denote as well

$$v \in \mathbb{U} :\Leftrightarrow (v_1, v_2) \in \mathbb{R}^4 \times \mathbb{R}^3, \qquad (54a)$$
$$v_1 \in \mathbb{R}^4 :\Leftrightarrow (U, \tau) \in \mathbb{R} \times \mathbb{R}^3, \qquad (54b)$$
$$v_2 \in \mathbb{R}^3 :\Leftrightarrow \tau_m \in \mathbb{R}^3, \qquad (54c)$$

where $v_1$ will be the input to one subsystem (thrust propelled), and $v_2$ will be the input to the other subsystem (unit vector double integrator).

Based on Fig. 6, consider then the mapping

$$f : \mathbb{X}\backslash_\sim \ni [x] \mapsto f([x]) \in \mathbb{Y} \tag{55}$$

$$f([x]) := \begin{bmatrix} \frac{mp+MP}{m+M} \\ \frac{mv+MV}{m+M} \\ Re_3 \\ \Pi\left(Re_3\right)R\Omega \\ \hline re_3 \\ \Pi\left(re_3\right)r\omega \end{bmatrix} \left( = \begin{bmatrix} p_{cm} \\ v_{cm} \\ n \\ \varpi \\ \hline r \\ \omega \end{bmatrix} = \begin{bmatrix} y_1 \\ \hline y_2 \end{bmatrix} \right),$$

with $\mathbb{Y}$ as defined in (52a), and consider as well the mapping

$$h : \mathbb{Y} \ni y \mapsto h(y) \in \mathbb{X}\backslash_\sim \tag{56}$$

$$h(y) := \begin{bmatrix} \begin{bmatrix} p_{cm} - l\frac{M}{m+M}r \\ \bar{r} \\ p_{cm} + l\frac{m}{m+M}r \\ \bar{R} \\ v_{cm} - l\frac{M}{m+M}\mathcal{S}\left(\omega\right)r \\ \bar{r}^T\omega \\ v_{cm} + l\frac{m}{m+M}\mathcal{S}\left(\omega\right)r \\ \bar{R}^T\varpi \end{bmatrix} \end{bmatrix} \left( = \begin{bmatrix} \begin{bmatrix} p \\ r \\ P \\ R \\ \hline v \\ \omega \\ V \\ \Omega \end{bmatrix} \end{bmatrix} = [x] \right).$$

$$\underbrace{\qquad\qquad\qquad}_{\substack{\bar{r}\in\mathbb{SO}(3),\bar{r}e_3=r \\ \bar{R}\in\mathbb{SO}(3),\bar{R}e_3=n}}$$

*Proposition 13:* The map $f$ in (55) is well defined, and

$$f \circ h = \mathrm{id}_\mathbb{Y} \quad \text{and} \quad h \circ f = \mathrm{id}_{\mathbb{X}\backslash_\sim}, \tag{57}$$

i.e., $h = f^{-1}$ and $f = h^{-1}$.

*Proof 4:* The map $f$ in (55) is defined with a representative of an equivalence class, so we must show that $f$ is independent of the choice of representative. Consider (31), and notice that

$$Re_3 = (RR_z(\theta))e_3, \text{ and that} \tag{58}$$
$$\Pi\left(Re_3\right)R\Omega = \Pi\left((RR_z(\theta))e_3\right)(RR_z(\theta))(R_z^T(\theta)\Omega), \tag{59}$$

which suffices to conclude that $f$ is independent of the choice of representative belonging to an equivalence class established by the equivalence relation in (36) (i.e., for any $x \in \mathbb{X}$ and for any $\bar{x}, \tilde{x} \in [x] \in \mathbb{X}\backslash_\sim$, $f([\bar{x}]) = f([\tilde{x}])$). The second part of the Proposition follows from straightforward computations. Let us just illustrate the identities in (57) for the component $\varpi$ of $f$ (denote it $f|_\varpi$) and the component $\Omega$ of $h$ (denote it $h|_\Omega$) – i.e., we verify that $f|_\varpi \circ h(y) = \varpi$ and that $h|_\Omega \circ f([x]) = [\Omega]$ (where, by the equivalence relation in (36), angular velocities are equivalent up to rotations around the third body axis and up to the third-component – i.e., $[\Omega] := [R_z(\theta_P)(\Omega + Be_3)]$ for any real $\theta_P$ and $B$). Then, notice that

$$f|_\varpi \circ h(y) = f|_\varpi(h(y)) \overset{(55)}{\equiv} \Pi\left(Re_3\right)R\Omega|_{R \text{ and } \Omega \text{ as in } (56)}$$
$$= \Pi\left(\bar{R}e_3\right)\bar{R}\bar{R}^T\varpi$$
$$\overset{\bar{R}\in\mathbb{SO}(3)}{=} \Pi\left(\bar{R}e_3\right)\varpi$$
$$\overset{(56):\bar{R}e_3=n}{=} \Pi\left(n\right)\varpi = (I_3 - nn^T)\varpi$$
$$\overset{(53):n^T\varpi=0}{=} \varpi.$$

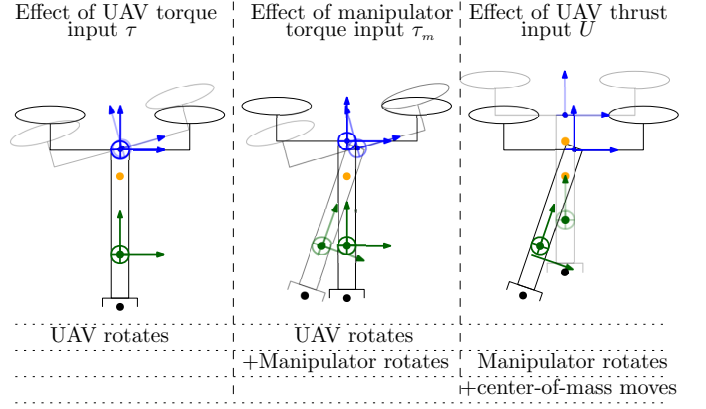

Fig. 7: Effects of original input $u = (U, \tau, \tau_m)$ in UAV-manipulator system.

Finally, notice that

$$h|_\Omega \circ f([x]) = h|_\Omega(f([x])) \overset{(56)}{\equiv} [\bar{R}^T\varpi]|_{\varpi \text{ as in } (55)}$$
$$= [\bar{R}^T\Pi\left(Re_3\right)R\Omega] = [\bar{R}^T R\Pi\left(e_3\right)\Omega]$$
$$\overset{\substack{Re_3\overset{(55)}{=}n\overset{(56)}{=}\bar{R}e_3\Rightarrow \\ \Rightarrow \bar{R}^T R=R_z^T(\theta_P) \text{ for some } \theta_P}}{=} [R_z^T(\theta_P)\Pi\left(e_3\right)\Omega]$$
$$\overset{(36):[\Omega]=[R_z(\theta_P)(\Omega+\Omega^T e_3 e_3)]}{=} [\Pi\left(e_3\right)\Omega + \Omega^T e_3 e_3]$$
$$= [\Omega].$$

The other identities are verified similarly (and are easier to verify).

*B. Input transformation and transformed vector field*

Let us construct the input transformation in two steps. For that purpose, consider the transformed dynamics with the original input (not the transformed input), which are given by

$$Df([x])X(x,u) = \begin{bmatrix} \frac{mv+MV}{m+M} \\ \frac{U}{m+M}Re_3 - ge_3 \\ \mathcal{S}\left(\Pi\left(Re_3\right)R\Omega\right)Re_3 \\ \Pi\left(Re_3\right)R(\star_1) \\ \hline \mathcal{S}\left(\Pi\left(re_3\right)r\omega\right)re_3 \\ \Pi\left(re_3\right)(\star_2) \end{bmatrix} \left( = \begin{bmatrix} \dot{p}_{cm} \\ \dot{v}_{cm} \\ \dot{n} \\ \dot{\varpi} \\ \hline \dot{r} \\ \dot{\omega} \end{bmatrix} \right), \tag{60}$$

$$(\star_1) = J^{-1}(\tau - R^T r\tau_m - \mathcal{S}\left(\Omega\right)J\Omega) - e_3^T\Omega\mathcal{S}\left(\Omega\right)e_3$$
$$(\star_2) = \frac{m+M}{l^2 mM}\frac{1}{\gamma}\left(\tau_m + \mathcal{S}\left(e_3\right)\left(\frac{mlU}{m+M}r^T Re_3 + j_{zz}e_3^T\omega\omega\right)\right).$$

If follows from (60) that the original input $u = (U, \tau, \tau_m)$ has the effects illustrated in Fig. 7. (i) The UAV torque input $\tau$ only makes the UAV rotate (not the manipulator). (ii) The manipulator torque input $\tau_m$ makes the manipulator rotate, but it also makes the UAV rotate (in an opposite direction, and with a different scaling – factor $\|J^{-1}R^T r\| = \|J^{-1}\|$ in $\star_1$ and factor $\frac{m+M}{l^2 mM}\frac{1}{\gamma}$ in $\star_2$). (iii) The UAV thrust input $U$ makes the whole system (i.e., its center-of-mass) accelerate along the UAV's third body axis; but it also produces a torque on the manipulator third axis, which makes it rotate. The previous discussion provides the basis for the design of the input transformation, whose idea is to design a UAV torque input $\tau$ that controls the UAV attitude by canceling the effect of the manipulator torque input $\tau_m$ on the UAV attitude; and

next, to design a manipulator torque input $\tau_m$ that controls the manipulator attitude by canceling the effect of the UAV thrust input $U$ on the manipulator's attitude (notice the design is made in a cascaded fashion). Consider then

$$\bar{u}_1^{cl} : \mathbb{X} \times \mathbb{U} \times \mathbb{R} \ni (x, u, \tau_\psi) \mapsto \bar{u}_1^{cl}(x, u, \tau_\psi) \in \mathbb{U} \qquad (61)$$

$$\bar{u}_1^{cl}(x, u, \tau_\psi) := \begin{bmatrix} (m+M)U \\ \left\{ \begin{array}{c} J(\Pi(e_3)R^T\tau + \tau_\psi e_3 + e_3^T\Omega\mathcal{S}(\Omega)e_3) + \\ + R^T r\tau_m + \mathcal{S}(\Omega)J\Omega \end{array} \right\} \\ \tau_m \end{bmatrix}$$

which when composed in (60) yields $\dot{v}_{cm} = URe_3 - ge_3$ and to $\dot{\varpi} = \Pi(Re_3)\tau$ (for the purpose of $\tau_\psi$ in (61), we ask the reader to await until Remark 15). Then consider

$$\bar{u}_2^{cl} : \mathbb{X} \times \mathbb{U} \ni (x, u, \tau_\psi) \mapsto \bar{u}_2^{cl}(x, u) \in \mathbb{U} \qquad (62)$$

$$\bar{u}_2^{cl}(x, u) := \begin{bmatrix} U \\ \tau \\ \left\{ \begin{array}{c} \frac{l^2 mM}{m+M}\gamma\Pi(e_3)r^T\tau_m - \\ -\mathcal{S}(e_3)\left(mlUr^TRe_3 + j_{zz}e_3^T\omega\omega\right) \end{array} \right\} \end{bmatrix}$$

which when composed in (60) (and after applying (61) first) it leads to $\dot{\omega} = \Pi(re_3)\tau_m$.

Consider then the input transformation as a composition of the previous control laws (61) and (62), i.e.,

$$\bar{u}^{cl} : \mathbb{X} \times \mathbb{U} \times \mathbb{R} \ni (x, u, \tau_\psi) \mapsto \bar{u}^{cl}(x, u, \tau_\psi) \in \mathbb{U} \qquad (63)$$
$$\bar{u}^{cl}(x, u, \tau_\psi) := \bar{u}_1^{cl}(x, \bar{u}_2^{cl}(x, u), \tau_\psi).$$

Given the input transformation in (63) and the state transformation in (55), one can then compute the transformed dynamics. In fact, it follows that composing (60) with the control law (63) results in

$$Df([x])X(x, \bar{u}^{cl}(x, u, \tau_\psi)) = \begin{bmatrix} \frac{mv+MV}{m+M} \\ URe_3 - ge_3 \\ \mathcal{S}(\Pi(Re_3)R\Omega)Re_3 \\ \Pi(Re_3)\tau \\ \hline \mathcal{S}(\Pi(re_3)r\omega)re_3 \\ \Pi(re_3)\tau_m \end{bmatrix} \qquad (64)$$

and as such the vector field in the new coordinates is given by

$$Y : \mathbb{Y} \times \mathbb{U} \ni (y, v) \mapsto Y(y, v) \in T_y\mathbb{Y} \qquad (65)$$
$$Y(y, v) := Df([x])X(x, \bar{u}^{cl}(x, v, \cdot))|_{x \in h(y)}$$

$$= \begin{bmatrix} Y_1(y_1, v_1) \\ \hline Y_2(y_2, v_2) \end{bmatrix} = \begin{bmatrix} v_{cm} \\ Un - ge_3 \\ \mathcal{S}(\varpi)n \\ \Pi(n)\tau \\ \hline \mathcal{S}(\omega)r \\ \Pi(r)\tau_m \end{bmatrix} \left( = \begin{bmatrix} \dot{p}_{cm} \\ \dot{v}_{cm} \\ \dot{n} \\ \dot{\varpi} \\ \hline \dot{r} \\ \dot{\omega} \end{bmatrix} = \begin{bmatrix} \dot{y}_1 \\ \hline \dot{y}_2 \end{bmatrix} \right),$$

and where we draw attention to the state and input decompositions in (53) and (54). It is now clear that the UAV-manipulator system can be understood as two decoupled systems, with vectors fields $Y_1$ and $Y_2$ (and for which controllers are found in the literature). Let us highlight the cascaded structure of those two vector fields (below, and for brevity, $0 \equiv 0_{3\times3}$ and

$I \equiv I_3$), which is better understood if they are rewritten as

$$Y_1(y_1, v_1) = \begin{bmatrix} 0 & I & 0 & 0 \\ 0 & 0 & UI & 0 \\ 0 & 0 & 0 & -\mathcal{S}(n) \\ 0 & 0 & 0 & 0 \end{bmatrix} \begin{bmatrix} p_{cm} \\ v_{cm} \\ n \\ \varpi \end{bmatrix} + \begin{bmatrix} 0_3 \\ -ge_3 \\ 0_3 \\ \Pi(n)\tau \end{bmatrix}, \qquad (66)$$

$$Y_2(y_2, v_2) = \begin{bmatrix} 0 & -\mathcal{S}(r) \\ 0 & 0 \end{bmatrix} \begin{bmatrix} r \\ \omega \end{bmatrix} + \begin{bmatrix} 0_3 \\ \Pi(r)\tau_m \end{bmatrix}. \qquad (67)$$

Recall then Problem 1, and notice that the vector field $Y_1$ is concerned with the motion of the center-of-mass of the system, while the vector field $Y_2$ is concerned with the angular position motion of the manipulator. This motivates us to introduce the desired center-of-mass position based on the desired manipulator linear and angular position ($p^\star$ and $r^\star$ in Problem 1), defined as

$$p_{cm}^\star : \mathbb{R} \ni t \mapsto p_{cm}^\star(t) := p^\star(t) + l\frac{M}{m+M}r^\star(t) \in \mathbb{R}^3 \quad (68)$$

and which, for reasons that are made clear next, we assume satisfies

$$p_{cm}^\star \in \mathcal{C}^4, \qquad (69a)$$
$$\sup_{t \in \mathbb{R}} \|p_{cm}^{\star(2)}(t) + ge_3\| > 0, \qquad (69b)$$
$$\sup_{t \in \mathbb{R}} p_{cm}^{\star(i)}(t) < \infty \text{ for } i \in \{2, 3, 4\}. \qquad (69c)$$

### C. Differential flatness

It follows from the cascaded structure of the vector field $Y_1$ in (66) that it is differentially flat with respect to the position of the center-of-mass. In fact, if we require $t \mapsto p_{cm}(t) := p_{cm}^\star(t)$, then we find two equilibria trajectories and two equilibria inputs, namely (below $y_{1\pm}^\star$ stands for the two solutions, namely $y_{1+}^\star$ and $y_{1-}^\star$)

$$y_{1\pm}^\star : \mathbb{R} \ni t \mapsto y_{1\pm}^\star(t) \in \mathbb{Y}_1 \qquad (70)$$

$$y_{1\pm}^\star(t) := \begin{bmatrix} p_{cm}^\star(t) \\ v_{cm}^\star(t) \\ n_\pm^\star(t) \\ \varpi^\star(t) \end{bmatrix} := \begin{bmatrix} p_{cm}^{\star(0)}(t) \\ p_{cm}^{\star(1)}(t) \\ \pm\frac{p_{cm}^{\star(2)}(t)+ge_3}{\|p_{cm}^{\star(2)}(t)+ge_3\|} \\ \mathcal{S}\left(\frac{p_{cm}^{\star(2)}(t)+ge_3}{\|p_{cm}^{\star(2)}(t)+ge_3\|}\right)\frac{p_{cm}^{\star(3)}(t)}{\|p_{cm}^{\star(2)}(t)+ge_3\|} \end{bmatrix},$$

and (below we use the definition of $\varpi^\star$ presented above)

$$v_{1\pm}^\star : \mathbb{R} \ni t \mapsto v_{1\pm}^\star(t) := \begin{bmatrix} \pm\|p_{cm}^{\star(2)}(t) + ge_3\| \\ \varpi^{\star(1)}(t) \end{bmatrix} \in \mathbb{R}^4. \quad (71)$$

At this point, it becomes clear the necessity of the constraints (69a), (69b). Since (70) and (71) require $p_{cm}^\star$ to be four times continuously differentiable, (69a) becomes clear. On the other hand, $y_{1\pm}^\star$ is only well defined if (69b) is satisfied. The existence of two equilibria is also clear intuitively: loosely speaking, for $y_{1+}^\star$ the UAV points upwards and its thrust is positive, and for $y_{1-}^\star$ the UAV points downwards and its thrust is negative (regardless, in both cases, the center-of-mass tracks the desired trajectory).

Similarly, it follows from the cascaded structure of the vector field $Y_2$ in (67) that it is differentially flat with respect to the angular position of the manipulator. In fact, if we require

$t \mapsto r(t) := r^\star(t)$, then we find two equilibria trajectories and one equilibria input, namely

$$\mathbb{R} \ni t \mapsto y_{2\pm}^\star(t) \in \mathbb{Y}_2 \qquad (72)$$

$$y_{2\pm}^\star(t) := \begin{bmatrix} r_\pm^\star(t) \\ \omega^\star(t) \end{bmatrix} := \begin{bmatrix} \pm r^{\star(0)}(t) \\ \mathcal{S}\left(r^{\star(0)}(t)\right) r^{\star(1)}(t) \end{bmatrix}$$

and

$$\mathbb{R} \ni t \mapsto v_2^\star(t) := \mathcal{S}\left(r^{\star(0)}(t)\right) r^{\star(2)}(t) \in \mathbb{R}^3. \qquad (73)$$

The equilibria $\{y_{1+}^\star, y_{1-}^\star\}$ and $\{y_{2+}^\star, y_{2-}^\star\}$ just defined allows us to compute four equilibria in the original system apart from rotations around the rigid bodies third axis; i.e., it allows us to compute four equilibria equivalence classes (which we denote by $\{[x]_{+,+}^\star, [x]_{-,+}^\star, [x]_{+,-}^\star, [x]_{-,-}^\star\}$), with the help of the map $h$ in (56), namely

$$[x]_{\pm,\mp}^\star : \mathbb{R} \ni t \mapsto [x]^\star(t) := h(y_{\pm,\mp}^\star) \in \mathbb{X} \backslash_\sim, \qquad (74)$$

$$y_{\pm,\mp}^\star : \mathbb{R} \ni t \mapsto y_{\pm,\mp}^\star(t) := (y_{1\pm}^\star(t), y_{2\mp}^\star(t)) \in \mathbb{Y}.$$

(Note that the first slot $\pm$ in $y_{\pm,(\cdot)}^\star$ is related to the equilibria $y_{1\pm}^\star$; and the second slot $\pm$ in $y_{(\cdot),\pm}^\star$ is related to the equilibria $y_{2\pm}^\star$.)

*Assumption 14:* With the equilibria $y_{1,\pm}^\star$ in (70) and $y_{2,\pm}^\star$ in (72) in mind, assume there exist controllers

$$v_1^{cl} : \mathbb{R} \times \mathbb{Y}_1 \to \mathbb{R}^4, \qquad (75)$$

$$v_2^{cl} : \mathbb{R} \times \mathbb{Y}_2 \to \mathbb{R}^3, \qquad (76)$$

that guarantee that along solutions of

$$\dot{y}_1(t) = Y_1(y_1(t), v_1^{cl}(t, y_1(t))), y_1(0) \in \mathbb{Y}_1,$$

$$\dot{y}_2(t) = Y_2(y_2(t), v_2^{cl}(t, y_2(t))), y_2(0) \in \mathbb{Y}_2,$$

it holds that

$$\lim_{t \to \infty} (y_1(t) - y_{1+}^\star(t)) = 0_{12} \text{ or } \lim_{t \to \infty} (y_1(t) - y_{1-}^\star(t)) = 0_{12},$$

$$\lim_{t \to \infty} (y_2(t) - y_{2+}^\star(t)) = 0_6 \text{ or } \lim_{t \to \infty} (y_2(t) - y_{2-}^\star(t)) = 0_6,$$

which in turn implies that

$$\lim_{t \to \infty} (p_{cm}(t) - p_{cm}^\star(t)) = 0_3,$$

$$\lim_{t \to \infty} (r(t) \pm r^\star(t)) = 0_3.$$

Assume as well that there exist non-empty $\mathbb{Y}_{1,0} \subset \mathbb{Y}_1$ and $\mathbb{Y}_{2,0} \subset \mathbb{Y}_2$ such that along solutions of

$$\dot{y}_1(t) = Y_1(y_1(t), v_1^{cl}(t, y_1(t))), y_1(0) \in \mathbb{Y}_{1,0},$$

$$\dot{y}_2(t) = Y_2(y_2(t), v_2^{cl}(t, y_2(t))), y_2(0) \in \mathbb{Y}_{2,0},$$

it holds that $y_{1+}^\star$ and $y_{2+}^\star$ are stable, and that

$$\lim_{t \to \infty} (y_1(t) - y_{1+}^\star(t)) = 0_{12}, \qquad (77a)$$

$$\lim_{t \to \infty} (y_2(t) - y_{2+}^\star(t)) = 0_6. \qquad (77b)$$

Finally, assume that these controllers render both equilibria trajectories $y_{1-}^\star$ and $y_{2-}^\star$ unstable.

Note that the vector field $Y_1$ in (65) is that of a VTOL vehicle, and thus we are able to leverage controllers from the literature to control the position of the center-of-mass [39]–[42]. Similarly, the vector field $Y_2$ in (65) is that of a second order system in the unit sphere, and thus we are able to leverage controllers from the literature to control the attitude of the manipulator [43]–[46]. As such, Assumption 14 is indeed satisfied (provided that the desired center-of-mass position trajectory satisfies the constraints in (69)), and we can leverage controllers that are found in the literature and which satisfy the requirements described in Assumption 14.

*Remark 15:* Define $g : \mathbb{X} \ni x \mapsto g := e_3^T \Omega \in \mathbb{R}$, and notice that

$$Dg(x)X(x, \bar{u}^{cl}(x, v, \tau_\psi)) = \tau_\psi$$

for any $(x, u, \tau_\psi) \in \mathbb{X} \times \mathbb{U} \times \mathbb{R}$. As such, given some positive gain $k > 0$, consider the control law

$$\tau_\psi^{cl} : \mathbb{R} \times \mathbb{X} \ni (t, x) \mapsto \tau_\psi^{cl}(t, x) \in \mathbb{R}$$

$$\tau_\psi^{cl}(t, x) := -kg(x) = -ke_3^T \Omega.$$

It then follows that, $t \mapsto e_3^T \dot{\Omega}(t) = -ke_3^T \Omega(t)$, which implies that $t \mapsto e_3^T \Omega(t) = e_3^T \Omega(0)e^{-kt}$ along solutions of the closed loop system. For simplicity, we shall assume that the chosen control law for the UAV yaw motion is always the one shown above, which guarantees only that the UAV does not asymptotically spin around its third axis (loosely speaking, it does not yaw asymptotically). More complex control laws may be chosen for $\tau^{cl}$, but none (including the one above) interferes with the motion of the equivalence class (i.e., with $t \mapsto [x(t)]$).

Let us then present the result that guarantees that Problem 1 is indeed solved. For that purpose, let Assumption 14 be satisfied, and construct the control law in the original system as a composition of the input transformation $\bar{u}^{cl}$ in (63) with the control laws presented in Assumption 14, i.e., (see Remark 15 for $\tau_\psi^{cl}$)

$$u^{cl} : \mathbb{R} \times \mathbb{X} \ni (t, x) \mapsto u^{cl}(t, x) \in \mathbb{R}^7$$

$$u^{cl}(t, x) = \bar{u}^{cl}(x, v^{cl}(t, y), \tau_\psi^{cl}(t, x))|_{y=f([x])} \qquad (78)$$

$$v^{cl}(t, y) := (v_1^{cl}(t, y_1), v_2^{cl}(t, y_2)),$$

which leads to the closed loop vector field

$$\mathbb{R} \times \mathbb{X} \ni (t, x) \mapsto X^{cl}(t, x) := X(x, u^{cl}(t, x)) \in T_x\mathbb{X}. \qquad (79)$$

*Theorem 16:* Consider the closed loop vector field $X^{cl}$ in (79), constructed under the assumption the controllers in Assumption 14 are provided. Then, along solutions of

$$\dot{x}(t) = X^{cl}(t, x(t)), [x(0)] \in h(\mathbb{Y}_{1,0} \times \mathbb{Y}_{2,0}), \qquad (80)$$

where $h(\mathbb{Y}_{1,0} \times \mathbb{Y}_{2,0}) := \{h(y) \in \mathbb{X} \backslash_\sim : y \in \mathbb{Y}_{1,0} \times \mathbb{Y}_{2,0}\}$, it follows that

$$\lim_{t \to \infty} d_{\mathbb{X} \backslash_\sim}([x(t)], [x]_{+,+}^\star(t)) = 0, \qquad (81)$$

where the equilibrium equivalence class $[x]_{+,+}^\star$ is defined in (74) and the metric $d_{\mathbb{X} \backslash_\sim}$ is defined in (38); i.e., it follows that Problem 1 is satisfied, where rotations of the rigid bodies around their third axes are ignored.

*Proof 5:* Since $[x(0)] \in h(\mathbb{Y}_{1,0} \times \mathbb{Y}_{2,0})$ it follows that $(y_1(0), y_2(0)) =: y(0) := f([x(0)]) \in \mathbb{Y}_{1,0} \times \mathbb{Y}_{2,0}$; moreover, if we apply the control law (78), then the conclusion (77) in Assumption 14 holds.
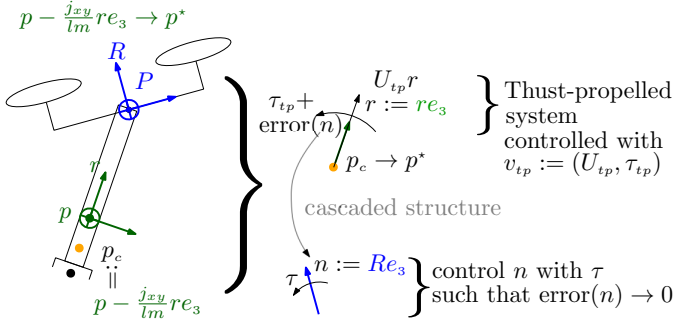
Fig. 8: By means of appropriate state and input transformations, the UAV-slung-manipulator may be understood as two systems in cascade: one thrust-propelled system followed by one unit-vector double-integrator system.

Because $t \mapsto y(t) = f([x(t)]) \Rightarrow t \mapsto [x(t)] = h(y(t))$, it follows that

$$
\begin{aligned}
& \lim_{t \to \infty} d_{\mathbb{X} \backslash \sim}([x(t)], [x]^{\star}_{+,+}(t)) = \\
&= \lim_{t \to \infty} d_{\mathbb{X} \backslash \sim}(h(y(t)), h(y^{\star}_{+,+}(t))) \\
&= \lim_{t \to \infty} d_{\mathbb{X} \backslash \sim}(h(y^{\star}_{+,+}(t) - y^{\star}_{+,+}(t) + y(t)), h(y^{\star}_{+,+}(t))) \\
{}_{h,d_{\mathbb{X} \backslash \sim} \in \mathcal{C}^{0}} &= \lim_{t \to \infty} d_{\mathbb{X} \backslash \sim}(h(y^{\star}_{+,+}(t) + \lim_{t \to \infty}(y(t) - y^{\star}_{+,+}(t))), h(y^{\star}_{+,+}(t))) \\
{}_{(77)} &= \lim_{t \to \infty} d_{\mathbb{X} \backslash \sim}(h(y^{\star}_{+,+}(t)), h(y^{\star}_{+,+}(t))) = 0,
\end{aligned}
$$

and where the limits above were derived by invoking continuity of the maps $h$ and $d_{\mathbb{X} \backslash \sim}$.

*Theorem 17:* Consider the closed loop vector field $X^{cl}$ in (79), constructed under the assumption the controllers in 14 are provided. Then, along solutions of

$$\dot{x}(t) = X^{cl}(t, x(t)), x(0) \in \mathbb{X}, \tag{82}$$

it follows that, for some equilibrium equivalence class $[x]^{\star}_{\star} \in \{[x]^{\star}_{+,+}, [x]^{\star}_{-,+}, [x]^{\star}_{+,-}, [x]^{\star}_{-,-}\}$,

$$\lim_{t \to \infty} d_{\mathbb{X} \backslash \sim}([x(t)], [x]^{\star}_{\star}(t)) = 0, \tag{83}$$

where the equilibria equivalence classes are defined in (74) and the metric $d_{\mathbb{X} \backslash \sim}$ is defined in (38); i.e., it follows that the position tracking problem in Problem 1 is satisfied while the orientation tracking is not necessarily satisfied. Moreover, the equilibria equivalence classes $[x]^{\star}_{-,+}$, $[x]^{\star}_{+,-}$ and $[x]^{\star}_{-,-}$ are all unstable.

*Proof 6:* The first part of the Theorem follows the same steps as in Theorem 16, and its proof is therefore omitted. For the instability of $[x]^{\star}_{-,+}$, $[x]^{\star}_{+,-}$ and $[x]^{\star}_{-,-}$ it suffices to invoke continuity of the map $h$.

## VII. UAV-SLUNG-MANIPULATOR

We shall verify next that the UAV-slung-manipulator system behaves as a thrust-propelled system followed/cascaded after a unit vector double integrator, as illustrated in Fig. 8. The three steps we follow next have been described in the Section V.

### A. State transformation

Recall the discussion from Section V. Let us then introduce the set $\mathbb{Y}$ defined as (you may read the subindex $tp$ as thrust-propelled)

$$\mathbb{Y}_{tp} := \{(p_c, v_c, r, \omega) \in (\mathbb{R}^3)^4 : r^T r = 1, r^T \omega = 0\}, \tag{84a}$$

$$\mathbb{Y} := \{(y_{tp}, n, \varpi) \in \mathbb{Y}_{tp} \times (\mathbb{R}^3)^2 : n^T n = 1, n^T \varpi = 0\}, \tag{84b}$$

with the inherited metrics $d_{\mathbb{Y}} := d_{\mathbb{R}^{18}}$ and $d_{\mathbb{Y}_{tp}} := d_{\mathbb{R}^{12}}$ (the set $\mathbb{Y}_{tp}$ will be used for the part of the system that resembles a thrust-propelled system – see Fig. 8). Hereafter, and for convenience, we decompose elements in the sets above as

$$y_{tp} \in \mathbb{Y}_{tp} :\Leftrightarrow (p_c, v_c, r, \omega) \in \mathbb{Y}_{tp}, \tag{85a}$$

$$y \in \mathbb{Y} :\Leftrightarrow (y_{tp}, n, \varpi) \in \mathbb{Y}. \tag{85b}$$

Hereafter, we denote as well

$$v_{tp} \in \mathbb{R}^4 :\Leftrightarrow (U_{tp}, \tau_{tp}) \in \mathbb{R} \times \mathbb{R}^3, \tag{86a}$$

$$v \in \mathbb{R}^4 :\Leftrightarrow (U_{tp}, \tau) \in \mathbb{R} \times \mathbb{R}^3, \tag{86b}$$

where $v_{tp}$ will be an auxiliary input (to the thrust propelled system), and $v$ will be the actual input to the whole system.

*Assumption 18:* We must at this point make the assumption that $e_3^T \omega(0) = 0$, i.e., that the manipulator is not initially spinning around itself (an alternative assumption would be to take $j_{zz} = 0$). Based on Proposition 3, it follows that $e_3^T \omega(t) = 0$ for all $t \in \mathbb{R}$, i.e., that the manipulator remains without spinning around itself, and thus, hereafter, and w.l.o.g., we restrict a state of the UAV-slung-manipulator system to be in the set $\{x \in \mathbb{X} : e_3^T \omega = 0\}$.

Recall the definition of the state space $\mathbb{X}$ in (52a), and the state decomposition in (15). Also, with Fig. 8 in mind, consider then the mapping

$$f : \mathbb{X} \backslash \sim \ni [x] \mapsto f([x]) \in \mathbb{Y} \tag{87}$$

$$
f([x]) := \begin{bmatrix} p - \frac{j_{xy}}{lm}re_3 \\ v - \frac{j_{xy}}{lm}r\mathcal{S}(\omega)e_3 \\ re_3 \\ \hdashline \Pi(re_3)r\omega \\ \bar{R}e_3 \\ \Pi(Re_3)R\Omega \end{bmatrix} \left( \begin{bmatrix} p_c \\ v_c \\ r \\ \omega \\ \hdashline n \\ \varpi \end{bmatrix} = \begin{bmatrix} y_{tp} \\ \hdashline n \\ \varpi \end{bmatrix} = y \right),
$$

and consider as well the mapping

$$h : \mathbb{Y} \ni y \mapsto h(y) \in \mathbb{X} \backslash \sim \tag{88}$$

$$
h(y) := \underbrace{\begin{bmatrix} \begin{bmatrix} p_c + \frac{j_{xy}}{lm}r \\ \tilde{r} \\ p_c + (\frac{j_{xy}}{lm}+l)r \\ R \\ \hdashline v_c + \frac{\tilde{j}_{xy}}{lm}\mathcal{S}(\omega)r \\ \tilde{r}^T\omega \\ v_c + (\frac{j_{xy}}{lm}+l)\mathcal{S}(\omega)r \\ \tilde{R}^T\varpi \end{bmatrix} \end{bmatrix}}_{\substack{\tilde{r} \in \mathbb{SO}(3), \tilde{r}e_3 = r \\ \tilde{R} \in \mathbb{SO}(3), \tilde{R}e_3 = n}} \left( \begin{bmatrix} \begin{bmatrix} p \\ r \\ P \\ R \\ \hdashline v \\ \omega \\ V \\ \Omega \end{bmatrix} \end{bmatrix} = [x] \right),
$$

*Proposition 19:* The map $f$ in (87) is well defined, and

$$f \circ h = \mathrm{id}_{\mathbb{Y}} \quad \text{and} \quad h \circ f = \mathrm{id}_{\mathbb{X} \backslash \sim}, \tag{89}$$

i.e., $h = f^{-1}$ and $f = h^{-1}$.

The proof follows the same steps as those in Proposition 13.

## B. Input transformation

Let us construct the input transformation in two steps. For that purpose, consider the transformed dynamics with the original input (not the transformed input), which are given by

$$Df([x])X(x,u) = \qquad (90)$$

$$= \begin{bmatrix} v - \frac{j_{xy}}{lm}r\mathcal{S}(\omega)e_3 \\ re_3(\star_1) - ge_3 \\ \mathcal{S}(\Pi(re_3)r\omega)re_3 \\ \frac{l}{j_{xy}}\mathcal{S}(re_3)rT(x,u) \\ \mathcal{S}(\Pi(Re_3)R\Omega)Re_3 \\ \Pi(Re_3)R(\star_2) \end{bmatrix} \left( \begin{bmatrix} \dot{p}_c \\ \dot{v}_c \\ \dot{r} \\ \dot{\omega} \\ \dot{\bar{n}} \\ \dot{\varpi} \end{bmatrix} = \begin{bmatrix} \dot{y}_{tp} \\ \cdot \\ \bar{n} \\ \dot{\varpi} \end{bmatrix} = \dot{y} \right),$$

$$(\star_1) = \frac{1}{m}(re_3)^T T(x,u) + \frac{j_{xy}}{lm}\omega^T\Pi(e_3)\omega,$$
$$(\star_2) = J^{-1}(\tau - \mathcal{S}(\Omega)J\Omega) - e_3^T\mathcal{S}(\Omega)e_3.$$

Equation (90) sheds some light into how to design the controller. Suppose for now that we had control over the internal tensions – $T(x,u)$ (which we do, by intermediate of the input $u$; however we do not have full control). Then, one can choose the component of those tensions aligned with the manipulator axis of axial symmetry (i.e.,$(re_3)^T T(x,u)$) in a way that behaves as a thrust in the differential equation $\dot{v}_c$ in (90); one can also choose the components of those tensions orthogonal to the manipulator's axis of axial symmetry (i.e., $\Pi(re_3)T(x,u)$) in a way that behaves as a torque on the manipulator axis of symmetry – see the differential equation $\dot{\omega}$ in (90). With the above in mind, and $\dot{v}_c$ and $\dot{\omega}$ in (90) also in mind, we define

$$T^{cl}: \mathbb{Y}_{tp} \times \mathbb{R}^4 \ni (y_{tp}, v_{tp}) \mapsto T^{cl}(y_{tp}, v_{tp}) \in \mathbb{R}^3,$$

$$T^{cl}(y_{tp}, v_{tp}) := \frac{1}{m}\left(U_{tp} - \frac{j_{xy}}{lm}\omega^T\omega\right)r - \frac{j_{xy}}{l}\mathcal{S}(r)\tau_{tp} \quad (91)$$

It then follows that

$$Df([x])X(x,u)|_{T(x,u)=T^{cl}(y_{tp},v_{tp})}|_{x\in h(y)} = \qquad (92)$$

$$= \begin{bmatrix} v_c \\ U_{tp}r - ge_3 \\ \mathcal{S}(\omega)r \\ \mathcal{S}(r)\tau_{tp} \\ \star \\ \star \end{bmatrix} \left( \begin{bmatrix} \dot{p}_c \\ \dot{v}_c \\ \dot{r} \\ \dot{\omega} \\ \dot{n} \\ \dot{\varpi} \end{bmatrix} \right).$$

(The equation above is strictly speaking ill-defined, specifically the last element $\dot{\varpi}$ depends on the choice of representative $x \in h(y) \in \mathbb{X}\backslash_\sim$; the correct formulation is found later in (104)).

However, we do not have full control over the internal tensions, which is simple to verify by inspecting of $T$ in (26): the tensions are three dimensional ($T(x,u) \in \mathbb{R}^3$), and the only input that acts on the tensions is the one-dimensional thrust ($U \in \mathbb{R}$). Moreover, by inspection of $T$ in (26), notice the affine dependence on $URe_3$, which motivates as to introduce an extra dummy variable $U_{3d}$ and such that $URe_3 = U_{3d} + (URe_3 - U_{3d})$; with this in mind, notice that $T(x,u)$ in (26) is equivalently written as (recall that in the UAV-slung-manipulator system $\tau_m = 0_3$ and $e_3^T\omega = 0$ – see

Assumption 18)

$$T(x,u) = \frac{rA_T^{-1}r^T}{M}\left(U_{3d} + lM\omega^T\omega re_3 + (URe_3 - U_{3d})\right), \qquad (93)$$

$$A_T \equiv \frac{m+M}{mM}I_3 + \frac{l^2}{j_{xy}}\Pi(e_3), \qquad (94)$$

Loosely speaking, since we wish that $T(x,u) = T^{cl}(y_{tp}, v_{tp})$, it naturally leads to the definition of

$$U_{3d}^{cl}: \mathbb{Y}_{tp} \times \mathbb{R}^4 \ni (y_{tp}, v_{tp}) \mapsto U_{3d}^{cl}(y_{tp}, v_{tp}) \in \mathbb{R}^3 \qquad (95)$$

$$U_{3d}^{cl}(y_{tp}, v_{tp}) := M\left(rA_T r^T T^{cl}(y_{tp}, v_{tp}) - l\omega^T\omega r\right)$$

$$\overset{(91)}{=} lM\gamma\left(\left(\frac{m+M}{M}\frac{U_{tp}}{l\gamma} - \omega^T\omega\right)r - \mathcal{S}(r)\tau_{tp}\right)$$

and, as such, if we take (93) with $U_{3d} = U_{3d}^{cl}(y_{tp}, v_{tp})$, it follows that the tensions $T(x,u)$ in (26) are equivalently written as

$$T(x,u) = T^{cl}(y_{tp}, v_{tp}) + \frac{rA_T^{-1}r^T}{M}(URe_3 - U_{3d}^{cl}(y_{tp}, v_{tp})), \qquad (96)$$

for any $x \in \mathbb{X}$ and any $v_{tp} \in \mathbb{R}^4$, and where $(y_{tp}, \star) = f([x])$ (see (87)). After simple computations, it then follows that for any $v_{tp} = (U_{tp}, \tau_{tp}) \in \mathbb{R}^4$,

$$Df([x])X(x,u)|_{T(x,u)\text{as in }(96)}|_{x\in h(y)} = \qquad (97)$$

$$= (92) + \begin{bmatrix} 0_{3\times3} \\ \frac{1}{m+M}rr^T \\ 0_{3\times3} \\ \frac{1}{lM\gamma}\mathcal{S}(r) \\ 0_{3\times3} \\ 0_{3\times3} \end{bmatrix} (Un - U_{3d}^{cl}(y_{tp}, v_{tp})) \left( = \begin{bmatrix} \dot{p}_c \\ \dot{v}_c \\ \dot{r} \\ \dot{\omega} \\ \dot{n} \\ \dot{\varpi} \end{bmatrix} \right).$$

A common and natural choice for the input $U$ in (97) is one that minimizes the error $Un - U_{3d}^{cl}(y_{tp}, u_{tp})$ in (97), i.e.,

$$\{n^T U_{3d}^{cl}(y_{tp}, v_{tp})\} = \arg\min_{U\in\mathbb{R}} \|Un - U_{3d}^{cl}(y_{tp}, v_{tp})\|. \qquad (98)$$

This choice, despite natural, is not ideal, since, if this choice is made, it results in

$$\dot{v}_c = U_{tp}r - ge_3 - \frac{1}{m+M}rr^T\Pi(n)U_{3d}^{cl}(y_{tp}, v_{tp}), \qquad (99)$$

which prevents us from using control laws in the literature which rely on the cascaded structure of the thrust-propelled system.

The other option (it comes at a cost we explain next) is one where $U$ is chosen such that the acceleration $\dot{v}_c$ in (97) depends solely on the thrust $U_{tp}$, i.e., such that $r^T(Un - U_{3d}^{cl}(y_{tp}, v_{tp}))$ vanishes. That leads to the definition of the control law

$$U^{cl}: \tilde{\mathbb{X}} \times \mathbb{U} \ni (x, U_{tp}) \mapsto U^{cl}(x, U_{tp}) \in \mathbb{R} \qquad (100)$$

$$U^{cl}(x, U_{tp}) := \frac{r^T U_{3d}^{cl}(y_{tp}, v_{tp})}{r^T n}\bigg|_{y=f([x])}$$

$$\overset{(95)}{=} \frac{(m+M)U_{tp} - lM\gamma\omega^T\omega}{(re_3)^T(Re_3)},$$

where

$$\tilde{\mathbb{X}} := \{x \in \mathbb{X} : (re_3)^T(Re_3) \neq 0\}. \qquad (101)$$

The cost of this choice is now clear: the control law is not defined in the whole state space; in fact, it is ill-defined when the manipulator arm is orthogonal to the thrust axis of the UAV. Notice, however, that, since the UAV and manipulator have physical volume, the manipulator should therefore never be orthogonal to the thrust axis of the UAV, since in this case the two rigid bodies would collide.

Again, after simple computations, it follows that for any $v_{tp} = (U_{tp}, \tau_{tp}) \in \mathbb{R}^4$,

$$Df([x])X(x,u)|_{U=U^{cl}(x,U_{tp})}|_{x \in h(y)} = \quad (102)$$

$$= (92) + \frac{1}{lM\gamma} \frac{\Pi(r)}{r^T n} \begin{bmatrix} 0_{3\times3} \\ 0_{3\times3} \\ 0_{3\times3} \\ I_{3\times3} \\ 0_{3\times3} \\ 0_{3\times3} \end{bmatrix} \mathcal{S}(n) U_{3d}^{cl}(y_{tp}, v_{tp}) \left( = \begin{bmatrix} \dot{p}_c \\ \dot{v}_c \\ \dot{r} \\ \dot{\omega} \\ \dot{n} \\ \dot{\varpi} \end{bmatrix} \right).$$

At this point, we can now introduce the input transformation. Consider then (see the input decomposition in (86))

$$\bar{u}^{cl} : \tilde{\mathbb{X}} \times \mathbb{U} \times \mathbb{R} \ni (x, v, \tau_\psi) \mapsto \bar{u}^{cl}(x, v, \tau_\psi) \in \mathbb{U} \quad (103)$$

$$\bar{u}^{cl}(x, v, \tau_\psi) := \begin{bmatrix} U^{cl}(x, U_{tp}) \\ J(\Pi(e_3) R\tau + \tau_\psi e_3 + e_3^T \Omega \mathcal{S}(\Omega) e_3) - \mathcal{S}(\Omega) J\Omega \end{bmatrix}.$$

Given the input transformation $\bar{u}^{cl}$ in (103) and the state transformation $f$ in (87) one can then compute the transformed dynamics. In fact, it follows that

$$Y : \mathbb{Y} \times \mathbb{U} \ni (y, v) \mapsto Y(y, v) \in T_y \mathbb{Y} \quad (104)$$

$$Y(y, v) := Df([x])X(x, \bar{u}^{cl}(x, v, \cdot))|_{x \in h(y)}$$

$$= \begin{bmatrix} v_c \\ U_{tp}r - ge_3 \\ \mathcal{S}(\omega) r \\ \frac{1}{r^T n} \left( \frac{(m+M)}{lM\gamma} U_{tp} - \omega^T \omega \right) \mathcal{S}(r) n \\ \mathcal{S}(\varpi) n \\ \Pi(n) \tau \end{bmatrix} \left( = \begin{bmatrix} \dot{p}_c \\ \dot{v}_c \\ \dot{r} \\ \dot{\omega} \\ \dot{n} \\ \dot{\varpi} \end{bmatrix} = \dot{y} \right)$$

which, for any $\tau_{tp} \in \mathbb{R}^3$, is exactly equivalent to

$$Y(y, v) = \begin{bmatrix} v_c \\ U_{tp}r - ge_3 \\ \mathcal{S}(\omega) r \\ \Pi(r) \tau_{tp} + \frac{\mathcal{S}(r)\mathcal{S}(n)U_{3d}^{cl}(y_{tp}, v_{tp})}{\gamma lMr^T n} \\ \mathcal{S}(\varpi) n \\ \Pi(n) \tau \end{bmatrix} \left( = \begin{bmatrix} \dot{p}_c \\ \dot{v}_c \\ \dot{r} \\ \dot{\omega} \\ \dot{n} \\ \dot{\varpi} \end{bmatrix} \right). \quad (105)$$

The cascaded structure of the this vector fields is now clear, since $Y$ can be equivalently written as (below, and for brevity, $0 \equiv 0_{3\times3}$ and $I \equiv I_3$)

$$Y(y, v) = \begin{bmatrix} 0 & I & 0 & 0 & 0 & 0 \\ 0 & 0 & U_{tp}I & 0 & 0 & 0 \\ 0 & 0 & 0 & -\mathcal{S}(r) & 0 & 0 \\ 0 & 0 & 0 & 0 & (\star)\mathcal{S}(r) & 0 \\ 0 & 0 & 0 & 0 & 0 & -\mathcal{S}(n) \\ 0 & 0 & 0 & 0 & 0 & 0 \end{bmatrix} \begin{bmatrix} p_c \\ v_c \\ r \\ \omega \\ n \\ \varpi \end{bmatrix} + \begin{bmatrix} 0_3 \\ -ge_3 \\ 0_3 \\ 0_3 \\ 0_3 \\ \Pi(n)\tau \end{bmatrix},$$

$$(\star) = \frac{1}{r^T n} \left( \frac{(m+M)}{\gamma} U_{tp} - \omega^T \omega \right).$$

Recall then Problem 2. For reasons that will be clear next, we require the desired position trajectory to satisfy some constraints, specifically

$$p^\star \in \mathcal{C}^6, \quad (106a)$$

$$\sup_{t \in \mathbb{R}} \|p^{\star(2)}(t) + ge_3\| > 0, \quad (106b)$$

$$\sup_{t \in \mathbb{R}} \left\{ \begin{array}{c} \|\Pi(r^\star(t))r^{\star(2)}(t)\|^2 + \\ \left( \pm \frac{1}{\gamma} \frac{(m+M)}{M} \frac{\|p^{\star(2)}(t)+ge_3\|}{l} - \|\mathcal{S}(r^\star(t))r^{\star(1)}(t)\|^2 \right)^2 \end{array} \right\} > 0, \quad (106c)$$

$$\sup_{t \in \mathbb{R}} p^{\star(i)}(t) < \infty \text{ for } i \in \{2, 3, 4, 5, 6\}, \quad (106d)$$

where $r^\star(t) \equiv \frac{p_c^{\star(2)}(t)+ge_3}{\|p_c^{\star(2)}(t)+ge_3\|}$.

Notice that the constraints (106) are satisfied for *non-aggressive* trajectories, i.e., for trajectories whose high-order derivatives of the position trajectory (in particular, $p^{\star(2)}, p^{\star(3)}, p^{\star(4)}$) are small in magnitude. In fact, if we take those high order derivatives to be zero (constant speed trajectory), the constraints (106b) and (106c) read as $\sup_{t \in \mathbb{R}} \|ge_3\| > 0$ and as $\sup_{t \in \mathbb{R}} \left( \pm \frac{1}{\gamma} \frac{(m+M)}{M} \frac{\|ge_3\|}{l} \right)^2 > 0$, which are indeed satisfied.

### C. Differential flatness

It follows from the cascaded structure of the vector field $Y$ in (104) that it is differentially flat with respect to the position $p_c$; equivalently, it follows that the vector field $X$ in (43) (if we ignore rotations of the rigid bodies around their third axes) is differentially flat with respect to the position $p - \frac{j_{xy}}{l^2 m} re_3$ (this justifies the claim in Remark 10). Indeed, if we require $t \mapsto p_c(t) := p^\star(t)$, then we find *four* equilibria state trajectories and *two* equilibria input trajectories, namely (below $y_{\pm,\mp}^\star$ stands for four solutions, namely $y_{+,+}^\star$, $y_{-,+}^\star$, $y_{+,-}^\star$ and $y_{-,-}^\star$)

$$y_{\pm,\mp}^\star : \mathbb{R} \ni t \mapsto y_{\pm,\mp}^\star(t) \in \mathbb{Y} \quad (107)$$

$$y_{\pm,\mp}^\star(t) := \begin{bmatrix} y_{tp,\pm}^\star \\ \hline n_{\pm,\mp}^\star(t) \\ \varpi^\star(t) \end{bmatrix} := \begin{bmatrix} p_c^\star(t) \\ v_c^\star(t) \\ r_\pm^\star(t) \\ \omega^\star(t) \\ \hline n_{\pm,\mp}^\star(t) \\ \varpi^\star(t) \end{bmatrix} := \begin{bmatrix} p^{\star(0)}(t) \\ p^{\star(1)}(t) \\ \pm\frac{p^{\star(2)}(t)+ge_3}{\|p^{\star(2)}(t)+ge_3\|} \\ \mathcal{S}(r_\pm^\star(t)) r_\pm^{\star(1)}(t) \\ \hline \mp\frac{U_{3d}^{cl}(y_{tp,\pm}^\star(t),u_{tp,\pm}^\star(t))}{\|U_{3d}^{cl}(y_{tp,\pm}^\star(t),u_{tp,\pm}^\star(t))\|} \\ \mathcal{S}(n_{\pm,\mp}^\star(t)) n_{\pm,\mp}^{\star(1)}(t) \end{bmatrix},$$

$$u_{tp,\pm}^\star(t) := \begin{bmatrix} U_{tp}^\star(t) \\ \tau_{tp}^\star(t) \end{bmatrix} := \begin{bmatrix} \pm\|p_c^{\star(2)}(t) + ge_3\| \\ \omega^{\star(1)}(t) \end{bmatrix},$$

and (below we use the definition of $\varpi^\star$ presented above)

$$v_\pm^\star : \mathbb{R} \ni t \mapsto v_\pm^\star(t) := \begin{bmatrix} \pm\|p_c^{\star(2)}(t) + ge_3\| \\ \varpi^{\star(1)}(t) \end{bmatrix} \in \mathbb{R}^4. \quad (108)$$

(Notice that, despite the presence of $r_\pm^\star$ and $n_{\pm,\mp}^\star$ in the definition of $\omega^\star$ and $\varpi^\star$ (respectively), these are independent of the choice of sign).

It should now be clear from (107), specifically from the definition of $r_\pm^\star$ and $n_{\pm,\mp}^\star$, why the desired position trajectory $p^\star$ was required to satisfy the constraints (106b) and (106c) (in particular, (106c) is equivalently expressed as $\sup_{t \in \mathbb{R}} \|U_{3d}^{cl}(y_{tp,\pm}^\star(t), u_{tp,\pm}^\star(t))\| > 0$). Intuitively, (106b) guarantees that the desired attitude of the manipulator third axis is well defined; and (106c) guarantees that the desired attitude of the UAV third axis is well defined.
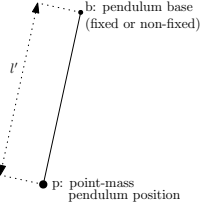
Fig. 9: Point mass pendulum with a fixed or moving base point.

The equilibria $\{y^\star_{+,+}, y^\star_{-,+}, y^\star_{+,-}, y^\star_{-,-}\}$ just defined allows us to compute four equilibria in the original system apart from rotations around the rigid bodies' third axis; i.e., it allows us to compute four equilibria equivalence classes (which we denote by $\{[x]^\star_{+,+}, [x]^\star_{-,+}, [x]^\star_{+,-}, [x]^\star_{-,-}\}$), with the help of the map $h$ in (88), namely

$$[x]^\star_{\pm,\mp} : \mathbb{R} \ni t \mapsto [x]^\star_{\pm,\mp}(t) := h(y^\star_{\pm,\mp}(t)) \in \mathbb{X}\backslash_\sim. \quad (109)$$

*Remark 20:* Consider a pendulum with a moving base, as illustrated in Fig. 9. The differential equations governing the motion of the pendulum are given by

$$\ddot{p} = \left( \frac{(p-b)^T}{l'} \frac{ge_3 + \ddot{b}}{l'} - \frac{\|\dot{p}-\dot{b}\|^2}{l'^2} \right) (p-b) - ge_3,$$

which implies that

$$\frac{\ddot{p} + ge_3}{\|\ddot{p} + ge_3\|} = \frac{p-b}{\|p-b\|} = \frac{p-b}{l'} \Leftrightarrow$$
$$\Leftrightarrow b = p + l' \frac{\ddot{p} + ge_3}{\|\ddot{p} + ge_3\|}. \quad (110)$$

Now, notice the UAV's as well as the manipulator's equilibrium positions are incorporated in the equilibrium equivalence class $[x]^\star_{+,+}$ in (109). Indeed it follows from the map $h$ in (88) and the equilibrium $y^\star_{+,+}$ in (107) that the equilibrium UAV's and manipulator's positions are given by

$$t \mapsto P^\star(t) = p^\star_c(t) + \left( \frac{j_{xy}}{lm} + l \right) \frac{\ddot{p}^\star_c(t) + ge_3}{\|\ddot{p}^\star_c(t) + ge_3\|},$$
$$t \mapsto p^\star(t) = p^\star_c(t) + \frac{j_{xy}}{lm} \frac{\ddot{p}^\star_c(t) + ge_3}{\|\ddot{p}^\star_c(t) + ge_3\|},$$

which, when compared with (110), explains why one should not specify a desired trajectory for the UAV's position, nor for the manipulator's position (unless $j_{xy} = 0$). Indeed, if one specifies a desired trajectory for the UAV's (or the manipulator's) position, then, there exist infinite equilibria equivalence class trajectories (rather than just four), where the manipulator behaves as a pendulum whose base is the UAV position (or the manipulator's) with a pendulum length $l' = \frac{j_{xy}}{lm} + l$ (or $l' = \frac{j_{xy}}{lm}$).

*Assumption 21:* With the equilibria $y^\star_{\pm,\mp}$ in (107) in mind, we assume there exists a controller

$$v^{cl} : \mathbb{R} \times \mathbb{Y} \to \mathbb{R}^4, \quad (111)$$

and non-empty $\mathbb{Y}_0 \subset \mathbb{Y}$, such that along solutions of

$$\dot{y}(t) = Y(y(t), v^{cl}(t, y(t))), y(0) \in \mathbb{Y}_0 \quad (112)$$

it holds that (i) $t \mapsto y(t)$ does not approach boundary of $\{y \in$

$\mathbb{Y} : r^T n > 0\}$; that (ii) $y^\star_{+,+}$ is stable; and that (iii)

$$\lim_{t \to \infty} (y(t) - y^\star_{+,+}(t)) = 0_{18}. \quad (113)$$

Finally, we assume that the equilibria trajectories $y^\star_{-,+}$, $y^\star_{+,-}$ and $y^\star_{-,-}$ are unstable.

Note that the vector field $Y$ in (105) is that of a VTOL vehicle cascaded after a second order system in the unit sphere. For this vector field, we are able to leverage controllers for VTOL vehicles from the literature [39]–[42], which must be complemented with two backstepping steps (related to the second order system). As such, Assumption 21 is indeed satisfied if the desired position trajectory satisfies the constraints in (106), i.e., a controller can be found that satisfies the conditions in the assumption.

Let us then present the result that guarantees that Problem 2 is indeed satisfied. For that purpose, let Assumption 21 be satisfied, and construct the control law in the original system as a composition of input transformation $\bar{u}^{cl}$ in (103) with the control law presented in Assumption 21, i.e., (see Remark 15 for $\tau^{cl}_\psi$)

$$u^{cl} : \mathbb{R} \times \mathbb{X} \ni (t,x) \mapsto u^{cl}(t,x) \in \mathbb{R}^4$$
$$u^{cl}(t,x) = \bar{u}^{cl}(x, v^{cl}(t,y), \tau^{cl}_\psi(t,x))|_{y=f([x])}, \quad (114)$$

which leads to the closed loop vector field

$$\mathbb{R} \times \mathbb{X} \ni (t,x) \mapsto X^{cl}(t,x) := X(x, u^{cl}(t,x)) \in T_x\mathbb{X}. \quad (115)$$

*Theorem 22:* Consider the closed loop vector field $X^{cl}$ in (115), constructed under the assumption that the controllers in Assumption 21 are provided. Then, along solutions of

$$\dot{x}(t) = X^{cl}(t, x(t)), [x(0)] \in h(\mathbb{Y}_0) \quad (116)$$

where $h(\mathbb{Y}_0) := \{h(y) \in \mathbb{X}\backslash_\sim : y \in \mathbb{Y}_0\}$, it follows that

$$\lim_{t \to \infty} d_{\mathbb{X}\backslash_\sim}([x(t)], [x]^\star_{+,+}(t)) = 0, \quad (117)$$

where the equilibrium equivalence class $[x]^\star_{+,+}$ is defined in (109) and the metric $d_{\mathbb{X}\backslash_\sim}$ is defined in (38). i.e., it follows that Problem 1 is satisfied, where rotations of the rigid bodies around their third axes is ignored. Moreover, the equilibria equivalence classes $[x]^\star_{-,+}$, $[x]^\star_{+,-}$ and $[x]^\star_{-,-}$ are all unstable.

*Proof 7:* Since $[x(0)] \in h(\mathbb{Y}_0)$ it follows that $y(0) := f([x(0)]) \in \mathbb{Y}_0$; moreover, if we apply the control law (114), then the conclusions in Assumption 21 hold. Because $t \mapsto y(t) = f([x(t)]) \Rightarrow t \mapsto [x(t)] = h(y(t))$, it follows that the same logic chain as in the proof of Theorem 16 follows, which completes the proof.

## VIII. SIMULATIONS

Let us provide simulations that illustrate the stability and convergence results presented. The physical constants were taken (in SI units) as $m = 0.3$, $M = 1.4$, $j = 0.007 \oplus 0.007 \oplus 0.001$ and $J = 0.01 \oplus 0.01 \oplus 0.2$; and with $l = 0.5$ for the UAV-manipulator system and with $l = 0.9$ for the UAV-slung-manipulator system. The specific control laws $v^{cl}$, as presented in Assumptions 14 and 21, are detailed in the mathematica files [49] (including the choice of gains; our particular choice of controller follows the structure described
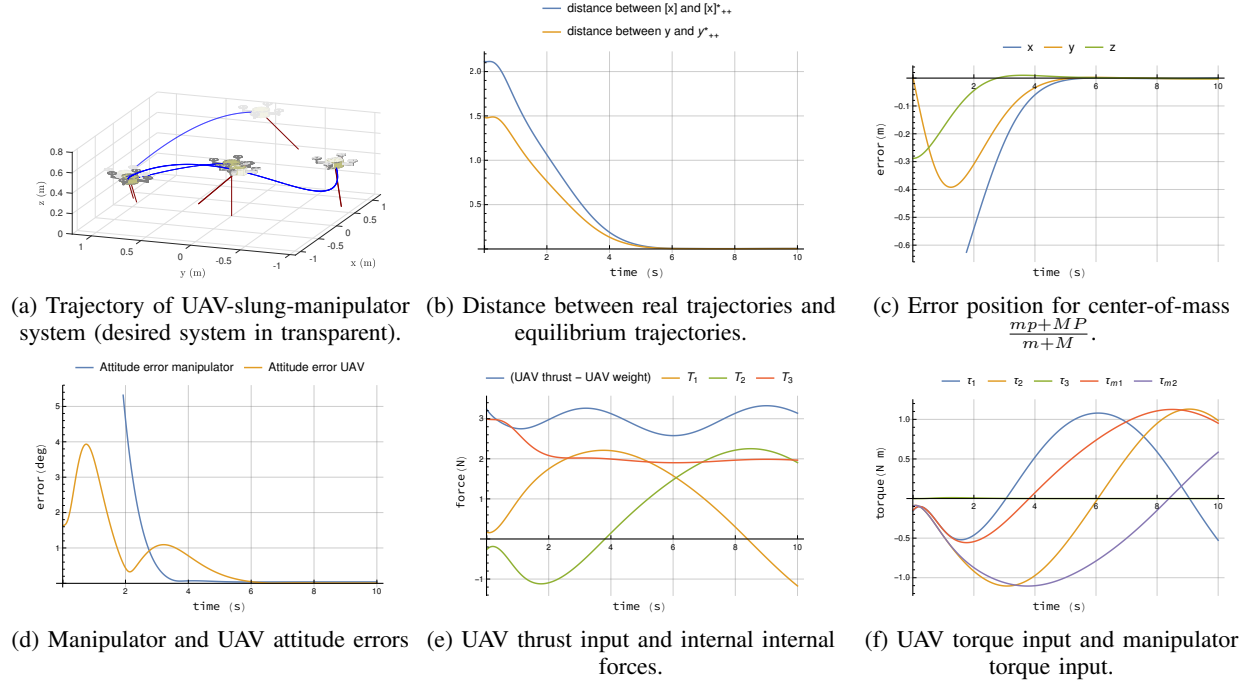
(a) Trajectory of UAV-slung-manipulator system (desired system in transparent).

(b) Distance between real trajectories and equilibrium trajectories.

(c) Error position for center-of-mass $\frac{mp+MP}{m+M}$.

(d) Manipulator and UAV attitude errors

(e) UAV thrust input and internal internal forces.

(f) UAV torque input and manipulator torque input.

Fig. 10: Simulation for UAV-manipulator system.



(a) Trajectory of UAV-slung-manipulator system (desired system in transparent).

(b) Distance between real trajectories and equilibrium trajectories.

(c) Error position for position $p - \frac{j_{xy}}{lm}re_3$.

(d) Manipulator and UAV attitude errors

(e) UAV thrust input and internal internal forces.
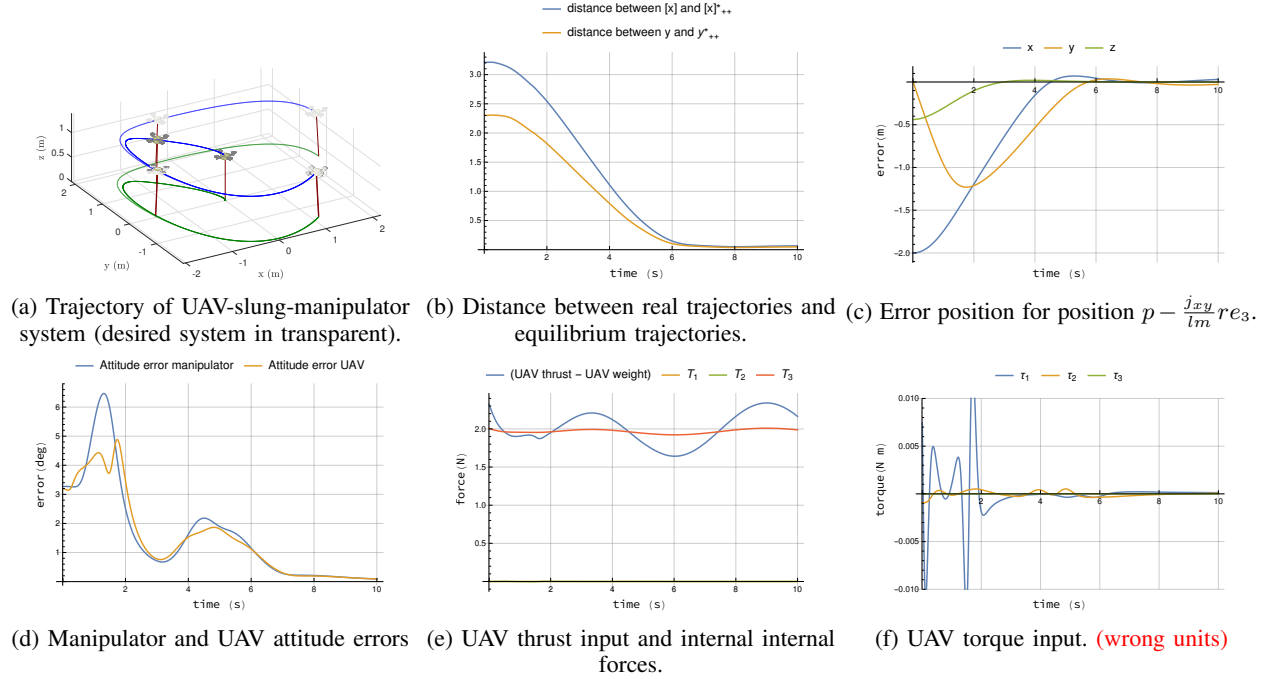
(f) UAV torque input. (wrong units)

Fig. 11: Simulation for UAV-slung-manipulator system.

in [42]). We provide two simulations, in Figs. 10 and 11, one for each system; these are obtained as the solution to $\dot{x}(t) = X^{cl}(t, x(t))$ with $x(0) = (0_3, I_3, le_3, I_3, 0_3, 0_3, 0_3, 0_3) \in \mathbb{X}$. For the desired position trajectory, we have chosen (Problems 1 and 2)

$$t \mapsto p^{\star}(t) := \left(2\cos\left(\tfrac{2\pi}{12}t\right), 2\sin\left(\tfrac{2\pi}{12}t\right), 0.2 + 0.2\cos\left(\tfrac{2\pi}{6}t\right)\right) \in \mathbb{R}^3, \tag{118}$$

corresponding to a circle of $2m$ radius in the horizontal plane and with a period of $12s$, superimposed with an oscillatory motion in the vertical direction with an amplitude of $0.2m$ and with a period of $6s$; and for the desired orientation trajectory, we have chosen (Problem 1)

$$t \mapsto r^{\star}(t) := \tfrac{2}{\sqrt{7}}\left(-\sin\left(\tfrac{2\pi}{12}t\right), \cos\left(\tfrac{2\pi}{12}t\right), \cos\left(\tfrac{\pi}{6}\right)\right) \in \mathbb{S}^2, \tag{119}$$

corresponding to an orientation trajectory where the desired manipulator is tilted $30°$ away from the vertical direction, and where the manipulator is tangent (when seen from the top) to the horizontal motion of $p^{\star}$.

Fig. 10 is related to the UAV-manipulator system, and Fig. 11 is related to the UAV-slung-manipulator system.

In Figs. 10a and 11a, one can visualize the real system pose (pose of both rigid bodies – the UAV's and the manipulator's) in opaque, and the equilibrium system pose in transparent. In Figs. 10b and 11b, one can visualize the distance between the equivalence-class trajectory $t \mapsto [x(t)]$ and the stable equilibrium equivalence-class trajectory $t \mapsto [x(t)]^{\star}_{+,+}$ as defined in (74) and (109), and by means of the metric $d_{\mathbb{X}\backslash\sim}$ defined in (38); as well as the distance between the transformed trajectory $t \mapsto y(t) := f(x(t))$ and the stable equilibrium transformed trajectory $t \mapsto y^{\star}_{+,+}(t)$ as defined in (74) and (107) (and by means of the metric $d_{\mathbb{Y}} := d_{\mathbb{R}^{18}}$). Notice that these distances may increase, during some time intervals, but they converge asymptotically to zero.

In Figs. 10c and 11c, the position error is shown for the positions of the thrust propelled systems, i.e., the center-of-mass position error ($t \mapsto \frac{mp(t)+MP(t)}{m+M} - p^{\star}_{cm}(t)$) for the UAV-manipulator system, and the position error $t \mapsto p(t) - \frac{j_{xy}}{lm}r(t)e_3 - p^{\star}(t)$ for the UAV-slung-manipulator system.

In Figs. 10d and 11d, the manipulator attitude error ($t \mapsto \arccos((r(t)e_3)^T r^{\star}_+(t))$), and the UAV attitude error ($t \mapsto \arccos((R(t)e_3)^T n^{\star}(t))$) are shown ($n^{\star} \equiv n^{\star}_+$ in Fig. 10d, and $n^{\star} \equiv n^{\star}_{+,+}$ in Fig. 11d).

In Figs. 10e–10f and Figs. 11e–11f, the input as obtained from the proposed control law $t \mapsto u^{cl}(t, x(t))$ is shown, with $u^{cl}$ as defined in (78) and in (114).

Finally, in Figs. 10e and 11e, the tensions forces $t \mapsto T(x(t), u^{cl}(t, x(t)))$ (with $T$ as defined in (26)) are shown. We emphasize only that the tension along the manipulator third axis is, in general, bigger than the others, since, loosely speaking, this is the component that needs to *cancel* the manipulator's weight.

## IX. CONCLUSIONS

This manuscript focuses on pose tracking problems for a system composed of two connected rigid bodies, namely an aerial vehicle – with hovering capabilities, and a rod-like rigid body. When a torque input at the joint connecting the two rigid bodies is available, a semi-pose tracking problem is formulated, requiring the rod object to track a desired pose trajectory. When no such torque input is available, a position tracking problem is formulated, requiring a specific point along the axis of axial symmetry of the rod object to track a desired position trajectory. Our approach for solving both these problems lied in finding a state and an input transformations, such that the vector field in the new coordinates is of a known form for which controllers are found in the literature, and which we leveraged in this manuscript.

## REFERENCES

[1] AEROWORKS aim. http://www.aeroworks2020.eu/.

[2] A. Wallar, E. Plaku, and D. A. Sofge. Reactive motion planning for unmanned aerial surveillance of risk-sensitive areas. *IEEE Transactions on Automation Science and Engineering*, 12(3):969–980, July 2015.

[3] A. Suarez, G. Heredia, and A. Ollero. Lightweight compliant arm with compliant finger for aerial manipulation and inspection. In *2016 IEEE/RSJ International Conference on Intelligent Robots and Systems (IROS)*, pages 4449–4454, Oct 2016.

[4] Markus Bernard, Konstantin Kondak, Ivan Maza, and Anibal Ollero. Autonomous transportation and deployment with aerial robots for search and rescue missions. *Journal of Field Robotics*, 28(6):914–931, 2011.

[5] I. Palunko, P. Cruz, and R. Fierro. Agile load transportation : Safe and efficient load manipulation with aerial robots. *IEEE Robotics Automation Magazine*, 19(3):69–79, Sept 2012.

[6] Konstantin Kondak, Markus Bernard, Fernando Caballero, Ivan Maza, and Anibal Ollero. Cooperative autonomous helicopters for load transportation and environment perception. *Advances in Robotics Research*, pages 299–310, 2009.

[7] M. Bisgaard, A. la Cour-Harbo, and J. D. Bendtsen. Adaptive control system for autonomous helicopter slung load operations. *Control Engineering Practice*, 18(7):800 – 811, 2010. Special Issue on Aerial Robotics.

[8] M. Gassner, T. Cieslewski, and D. Scaramuzza. Dynamic collaboration without communication: Vision-based cable-suspended load transport with two quadrotors. In *2017 IEEE International Conference on Robotics and Automation (ICRA)*, pages 5196–5202, May 2017.

[9] I. Palunko, A. Faust, P. Cruz, L. Tapia, and R. Fierro. A reinforcement learning approach towards autonomous suspended load manipulation using aerial robots. In *2013 IEEE International Conference on Robotics and Automation*, pages 4896–4901, May 2013.

[10] P. Cruz and R. Fierro. Autonomous lift of a cable-suspended load by an unmanned aerial robot. In *2014 IEEE Conference on Control Applications (CCA)*, pages 802–807, Oct 2014.

[11] P. J. Cruz, M. Oishi, and R. Fierro. Lift of a cable-suspended load by a quadrotor: A hybrid system approach. In *2015 American Control Conference (ACC)*, pages 1887–1892, July 2015.

[12] F. A. Goodarzi and T. Lee. Dynamics and control of quadrotor uavs transporting a rigid body connected via flexible cables. In *2015 American Control Conference (ACC)*, pages 4677–4682, July 2015.

[13] T. Lee, K. Sreenath, and V. Kumar. Geometric control of cooperating multiple quadrotor uavs with a suspended payload. In *52nd IEEE Conference on Decision and Control*, pages 5510–5515, Dec 2013.

[14] T. Lee. Collision avoidance for quadrotor uavs transporting a payload via voronoi tessellation. In *2015 American Control Conference (ACC)*, pages 1842–1848, July 2015.

[15] I. H. B. Pizetta, A. S. Brandão, and M. Sarcinelli-Filho. Modelling and control of a pvtol quadrotor carrying a suspended load. In *2015 International Conference on Unmanned Aircraft Systems (ICUAS)*, pages 444–450, June 2015.

[16] Nathan Michael, Jonathan Fink, and Vijay Kumar. Cooperative manipulation and transportation with aerial robots. *Autonomous Robots*, 30(1):73–86, 2011.

[17] Khelifa Baizid, G Giglio, Francesco Pierri, Miguel Angel Trujillo, Gianluca Antonelli, Fabrizio Caccavale, Antidio Viguria, Stefano Chiaverini, and Aníbal Ollero. Behavioral control of unmanned aerial vehicle manipulator systems. *Autonomous Robots*, 41(5):1203–1220, 2017.

[18] S. Kim, S. Choi, and H. J. Kim. Aerial manipulation using a quadrotor with a two dof robotic arm. In *2013 IEEE/RSJ International Conference on Intelligent Robots and Systems*, pages 4990–4995, Nov 2013.

[19] H. Lee, H. Kim, and H. J. Kim. Planning and control for collision-free cooperative aerial transportation. *IEEE Transactions on Automation Science and Engineering*, PP(99):1–13, 2017.

[20] H. Kim, H. Lee, S. Choi, Y. k. Noh, and H. J. Kim. Motion planning with movement primitives for cooperative aerial transportation in obstacle environment. In *2017 IEEE International Conference on Robotics and Automation (ICRA)*, pages 2328–2334, May 2017.

[21] M. Tognon, B. Yüksel, G. Buondonno, and A. Franchi. Dynamic decentralized control for protocentric aerial manipulators. In *2017 IEEE International Conference on Robotics and Automation (ICRA)*, pages 6375–6380, May 2017.

[22] F. Ruggiero et al. A multilayer control for multirotor UAVs equipped with a servo robot arm. In *International Conference on Robotics and Automation*, pages 4014–4020. IEEE, 2015.

[23] A. Jimenez-Cano, J. Martin, G. Heredia, A. Ollero, and R. Cano. Control of an aerial robot with multi-link arm for assembly tasks. In *International Conference on Robotics and Automation*, pages 4916–4921. IEEE, 2013.

[24] C. Korpela, M. Orsag, M. Pekala, and P. Oh. Dynamic stability of a mobile manipulating unmanned aerial vehicle. In *International Conference on Robotics and Automation*, pages 4922–4927, 2013.

[25] S. J. Lee and H. J. Kim. Autonomous swing-angle estimation for stable slung-load flight of multi-rotor uavs. In *2017 IEEE International Conference on Robotics and Automation (ICRA)*, pages 4576–4581, May 2017.

[26] S. Kim, S. Choi, H. Lee, and H. J. Kim. Vision-based collaborative lifting using quadrotor uavs. In *2014 14th International Conference on Control, Automation and Systems (ICCAS 2014)*, pages 1169–1174, Oct 2014.

[27] J. Thomas, G. Loianno, K. Sreenath, and V. Kumar. Toward image based visual servoing for aerial grasping and perching. In *2014 IEEE International Conference on Robotics and Automation (ICRA)*, pages 2113–2118, May 2014.

[28] R. Mebarki, V. Lippiello, and B. Siciliano. Toward image-based visual servoing for cooperative aerial manipulation. In *2015 IEEE International Conference on Robotics and Automation (ICRA)*, pages 6074–6080, May 2015.

[29] K. Sreenath, T. Lee, and V. Kumar. Geometric control and differential flatness of a quadrotor uav with a cable-suspended load. In *52nd IEEE Conference on Decision and Control*, pages 2269–2274, Dec 2013.

[30] K. Sreenath, N. Michael, and V. Kumar. Trajectory generation and control of a quadrotor with a cable-suspended load - a differentially-flat hybrid system. In *IEEE International Conference on Robotics and Automation*, pages 4888–4895. IEEE, 2013.

[31] I. Palunko, R. Fierro, and P. Cruz. Trajectory generation for swing-free maneuvers of a quadrotor with suspended payload: A dynamic programming approach. In *2012 IEEE International Conference on Robotics and Automation*, pages 2691–2697, May 2012.

[32] M. Tognon and A. Franchi. Dynamics, control, and estimation for aerial robots tethered by cables or bars. *IEEE Transactions on Robotics*, 33(4):834–845, Aug 2017.

[33] S. Tang and V. Kumar. Mixed integer quadratic program trajectory generation for a quadrotor with a cable-suspended payload. In *2015 IEEE International Conference on Robotics and Automation (ICRA)*, pages 2216–2222, May 2015.

[34] Patricio J. Cruz and Rafael Fierro. Cable-suspended load lifting by a quadrotor uav: hybrid model, trajectory generation, and control. *Autonomous Robots*, 41(8):1629–1643, Dec 2017.

[35] N. Chaturvedi and H. McClamroch. Asymptotic stabilization of the inverted equilibrium manifold of the 3-d pendulum using non-smooth feedback. *IEEE Transactions on Automatic Control*, 54(11):2658–2662, Nov 2009.

[36] N. A. Chaturvedi, N. H. McClamroch, and D. S. Bernstein. Asymptotic smooth stabilization of the inverted 3-d pendulum. *IEEE Transactions on Automatic Control*, 54(6):1204–1215, June 2009.

[37] A. S. Shiriaev, L. B. Freidovich, and M. W. Spong. Controlled invariants and trajectory planning for underactuated mechanical systems. *IEEE Transactions on Automatic Control*, 59(9):2555–2561, Sept 2014.

[38] M. W. Spong and R. Ortega. On adaptive inverse dynamics control of rigid robots. *IEEE Transactions on Automatic Control*, 35(1):92–95, Jan 1990.

[39] Minh-Duc Hua, Tarek Hamel, Pascal Morin, and Claude Samson. Introduction to feedback control of underactuated vtolvehicles: A review of basic control design ideas and principles. *IEEE Control Systems*, 33(1):61–75, 2013.

[40] R. Naldi, M. Furci, R. G. Sanfelice, and L. Marconi. Robust global trajectory tracking for underactuated vtol aerial vehicles using inner-outer loop control paradigms. *IEEE Transactions on Automatic Control*, 62(1):97–112, Jan 2017.

[41] M. D. Hua, T. Hamel, P. Morin, and C. Samson. A control approach for thrust-propelled underactuated vehicles and its application to vtol drones. *IEEE Transactions on Automatic Control*, 54(8):1837–1853, Aug 2009.

[42] P. O. Pereira and D. V. Dimarogonas. Lyapunov-based generic controller design for thrust-propelled underactuated systems. In *2016 European Control Conference (ECC)*, pages 594–599, June 2016.

[43] J. T. Y. Wen and K. Kreutz-Delgado. The attitude control problem. *IEEE Transactions on Automatic Control*, 36(10):1148–1162, Oct 1991.

[44] C. G. Mayhew, R. G. Sanfelice, and A. R. Teel. On path-lifting mechanisms and unwinding in quaternion-based attitude control. *IEEE Transactions on Automatic Control*, 58(5):1179–1191, May 2013.

[45] C. G. Mayhew, R. G. Sanfelice, and A. R. Teel. Quaternion-based hybrid control for robust global attitude tracking. *IEEE Transactions on Automatic Control*, 56(11):2555–2566, Nov 2011.

[46] S. P. Bhat. Controllability of nonlinear time-varying systems: applications to spacecraft attitude control using magnetic actuation. *IEEE Transactions on Automatic Control*, 50(11):1725–1735, Nov 2005.

[47] P. O. Pereira, R. Zanella, and D. V. Dimarogonas. Decoupled design of controllers for aerial manipulation with quadrotors. In *2016 IEEE/RSJ International Conference on Intelligent Robots and Systems (IROS)*, pages 4849–4855, Oct 2016.

[48] P. O. Pereira, M. Herzog, and D. V. Dimarogonas. Slung load transportation with a single aerial vehicle and disturbance removal. In *2016 24th Mediterranean Conference on Control and Automation (MED)*, pages 671–676, June 2016.

[49] P. Pereira and Dimos V. Dimarogonas. Mathematica files used in obtaining the manuscript's results. In *https://github.com/KTH-SML/aerial-generalized-slung-load-transportation.git*.

**Pedro Pereira** received the MSc degree in Aerospace Engineering from the Instituto Superior Técnico (IST) and the Delft University of Technology (TU Delft) in 2013. He is currently a PhD candidate at the department of Automatic Control in the Royal Institute of Technology (KTH). His research interests include nonlinear control and analysis, control of and motion planning for aerial vehicles, and multi-agent systems.

**Dimos Dimarogonas** was born in Athens, Greece, in 1978. He received the Diploma in Electrical and Computer Engineering in 2001 and the Ph.D. in Mechanical Engineering in 2007, both from the National Technical University of Athens (NTUA), Greece. Between May 2007 and February 2009, he was a Postdoctoral Researcher at the Automatic Control Laboratory, School of Electrical Engineering, ACCESS Linnaeus Center, KTH Royal Institute of Technology, Stockholm, Sweden. Between February 2009 and March 2010, he was a Postdoctoral Associate at the Laboratory for Information and Decision Systems (LIDS) at the Massachusetts Institute of Technology (MIT), Boston, MA, USA. He is currently an Associate Professor at the Automatic Control Laboratory, ACCESS Linnaeus Center, KTH Royal Institute of Technology, Stockholm, Sweden. His current research interests include Multi-Agent Systems, Hybrid Systems and Control, Robot Navigation and Networked Control. He was awarded a Docent in Automatic Control from KTH in 2012. He serves in the Editorial Board of Automatica, the IEEE Transactions on Automation Science and Engineering and the IET Control Theory and Applications and is a member of IEEE and the Technical Chamber of Greece. He received an ERC Starting Grant from the European Commission for the proposal BUCOPHSYS in 2014 and was awarded a Wallenberg Academy Fellow grant in 2015.